

## THE IMPOSSIBLY EARLY GALAXY PROBLEM

CHARLES. L. STEINHARDT<sup>1,2</sup>, PETER CAPAK<sup>1,2</sup>, DAN MASTERS<sup>1,2</sup>, JOSH S. SPEAGLE<sup>3,2</sup>*Draft version June 5, 2015*

## ABSTRACT

The current hierarchical merging paradigm and  $\Lambda$ CDM predict that the  $z \sim 4 - 8$  universe should be a time in which the most massive galaxies are transitioning from their initial halo assembly to the later baryonic evolution seen in star-forming galaxies and quasars. However, no evidence of this transition has been found in many high redshift galaxy surveys including CFHTLS, CANDELS and SPLASH, the first studies to probe the high-mass end at these redshifts. Indeed, if halo mass to stellar mass ratios estimated at lower-redshift continue to  $z \sim 6 - 8$ , CANDELS and SPLASH report several orders of magnitude more  $M \sim 10^{12-13} M_{\odot}$  halos than are possible to have formed by those redshifts, implying these massive galaxies formed impossibly early. We consider various systematics in the stellar synthesis models used to estimate physical parameters and possible galaxy formation scenarios in an effort to reconcile observation with theory. Although known uncertainties can greatly reduce the disparity between recent observations and cold dark matter merger simulations, even taking the most conservative view of the observations, there remains considerable tension with current theory.

*Subject headings:* galaxies: evolution

arXiv 1506.01377

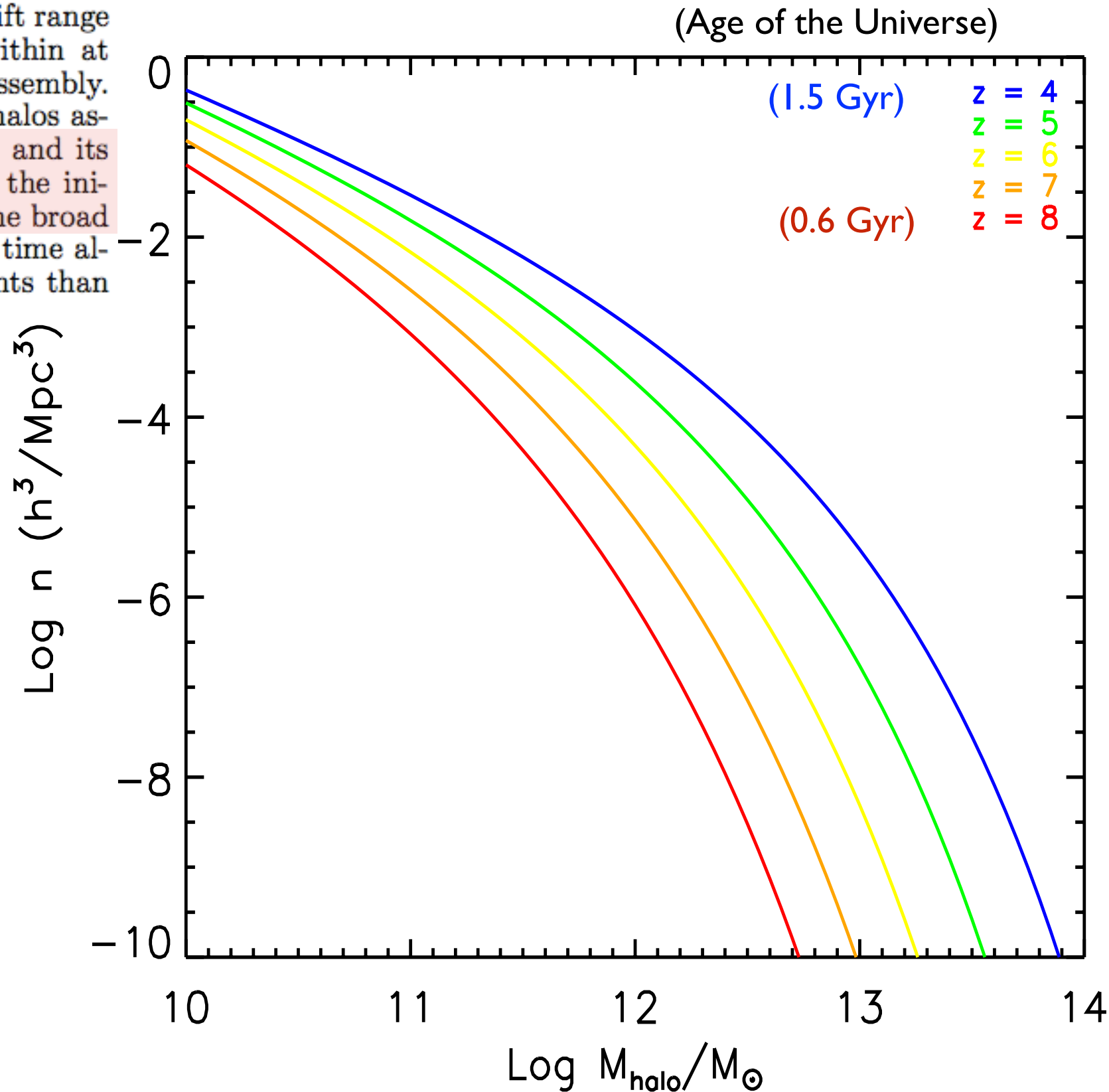
<sup>1</sup> California Institute of Technology, MC 105-24, 1200 East California Blvd., Pasadena, CA 91125, USA

<sup>2</sup> Infrared Processing and Analysis Center, California Institute of Technology, MC 100-22, 770 South Wilson Ave., Pasadena, CA 91125, USA

<sup>3</sup> Harvard University Department of Astronomy, 60 Garden St., MS 46, Cambridge, MA 02138, USA

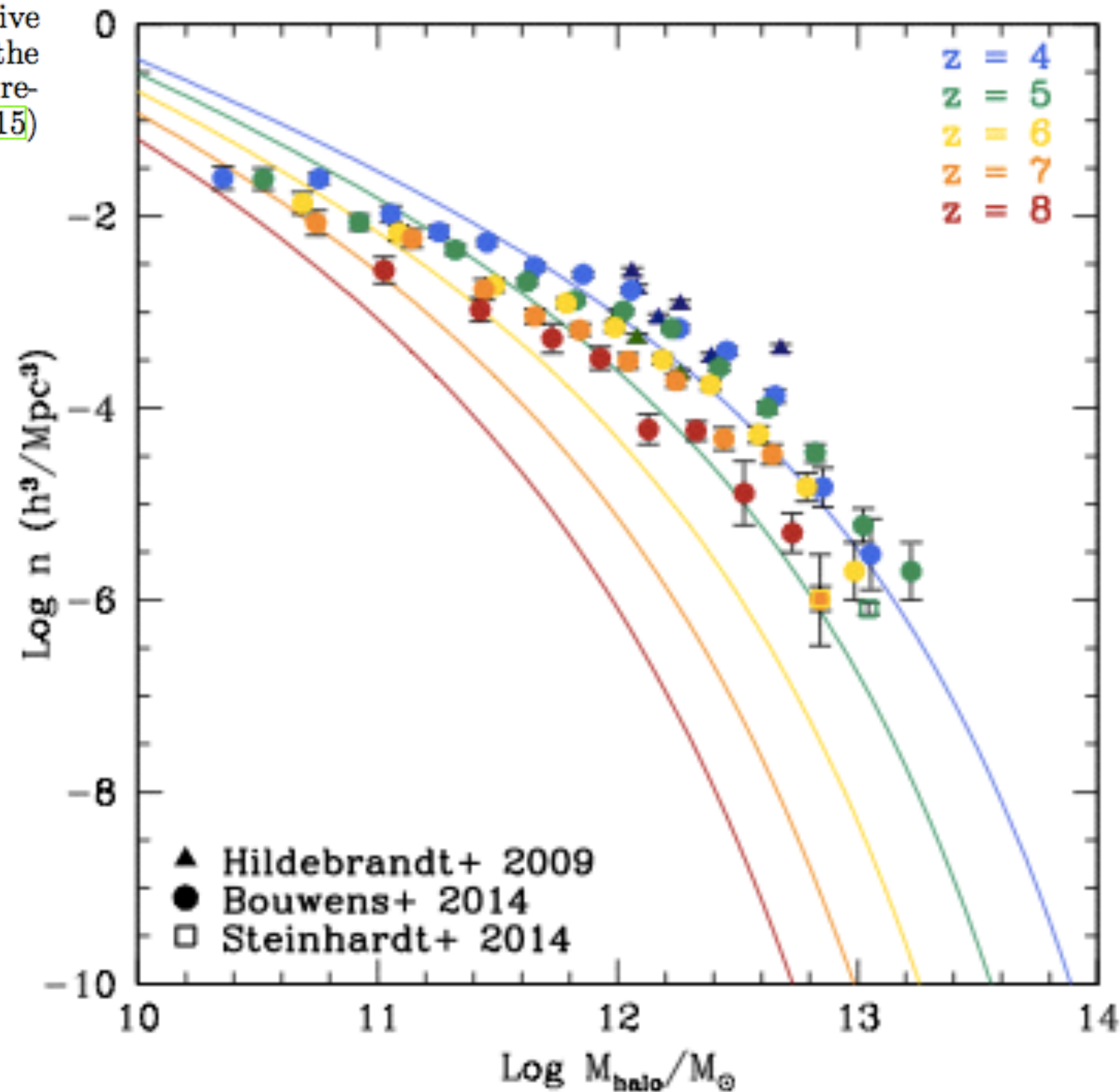
# Halo mass function evolution at $4 < z < 8$

In the consensus  $\Lambda$ CDM model, the high-mass end of the predicted halo mass function changes rapidly between  $z \sim 8 - 4$ , with halos containing the most massive galaxies typically virializing towards  $z = 4$  (e.g., Sheth et al. (2001)). The timespan of 0.9 Gyr over this redshift range means that we likely observe these galaxies within at most a few dynamical times of their initial assembly. Since galaxies are expected to form after their halos assemble, the number density of massive systems and its redshift evolution can provide a good probe of the initial formation of their dark matter halos. The broad redshift range over a relatively small amount of time allows for more precise cosmic epoch measurements than are easily obtainable at lower redshift.



# « Data » versus model

compiled in Figure 1, showing the large and diverging disagreement between the theoretical and observational evolution of the halo mass function at high redshift. Specifically, we find that observational halo mass function estimates correspond to a higher number density of massive halos than should have been able to form through the rapid collapse and evolution of rare, highly-overdense regions (Fig. 1). The analysis of Finkelstein et al. (2015)

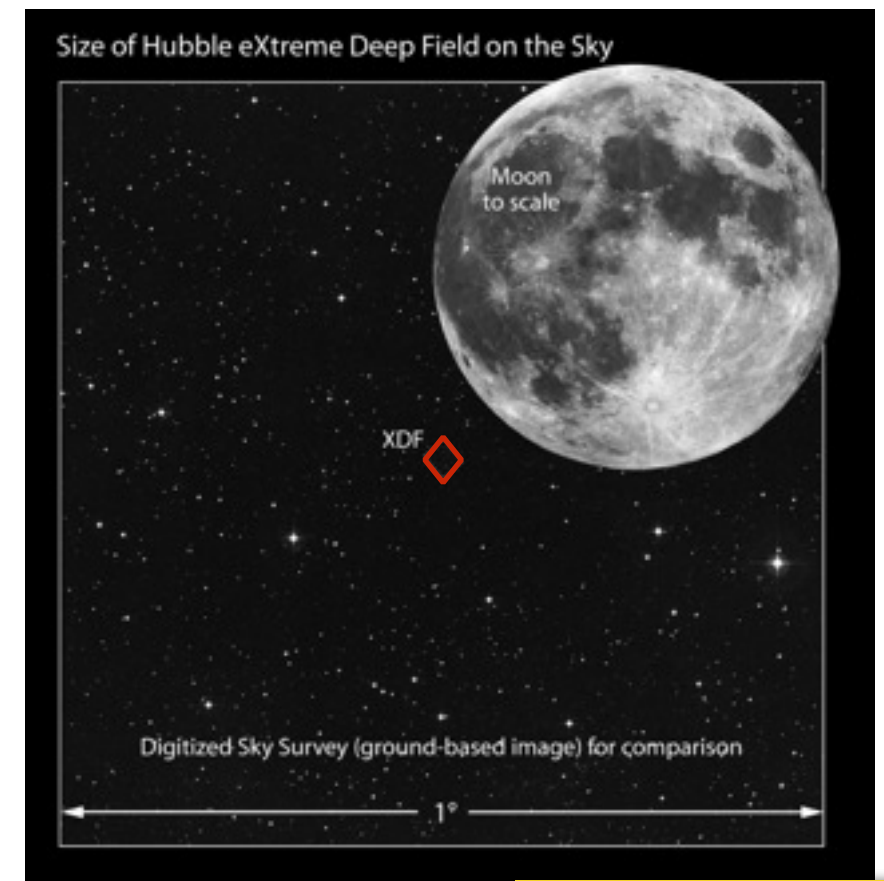
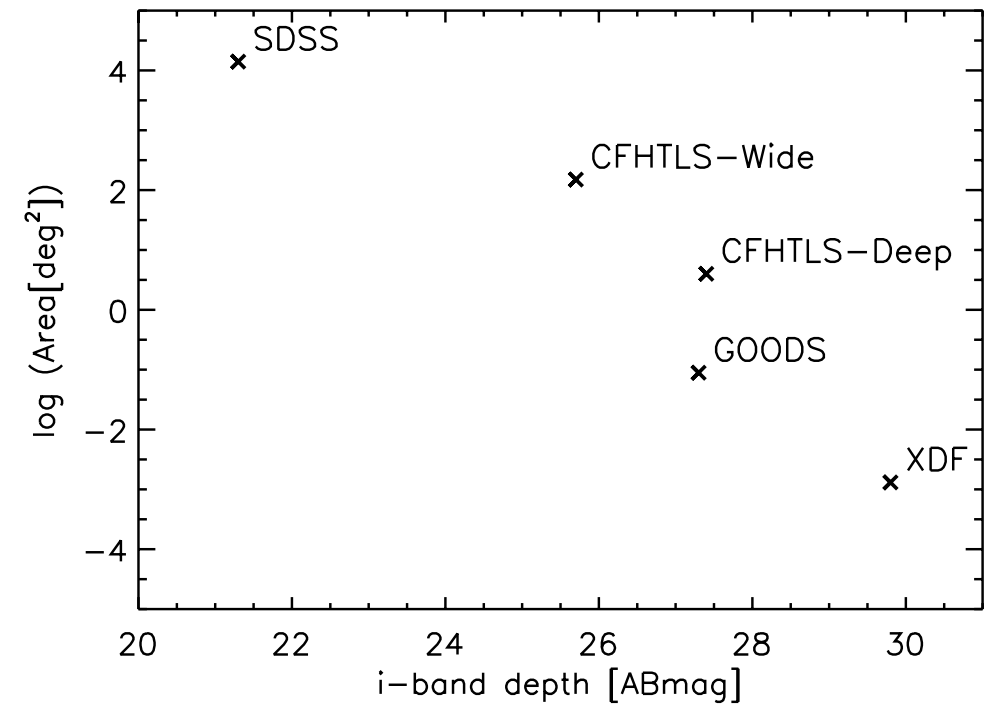
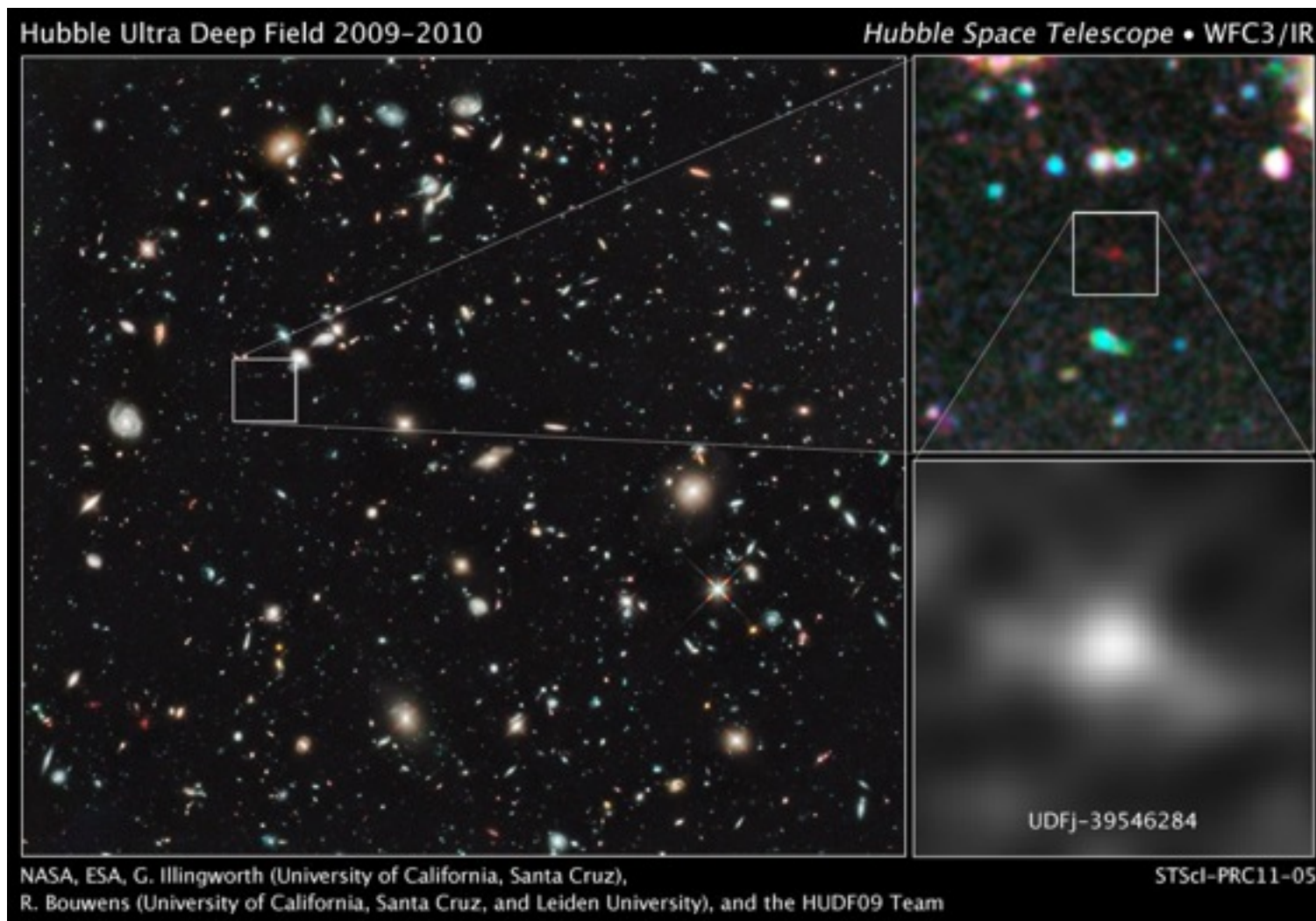


# Observations to select $4 < z < 8$ galaxies

## Observations requirements

- multi-wavelength coverage
- deep imaging ( $\rightarrow$  limited to small areas)
- « large » area (massive galaxies are rare)

FI05W: 18.6 hours  
FI25W: 27.8 hours  
FI60W: 40.8 hours



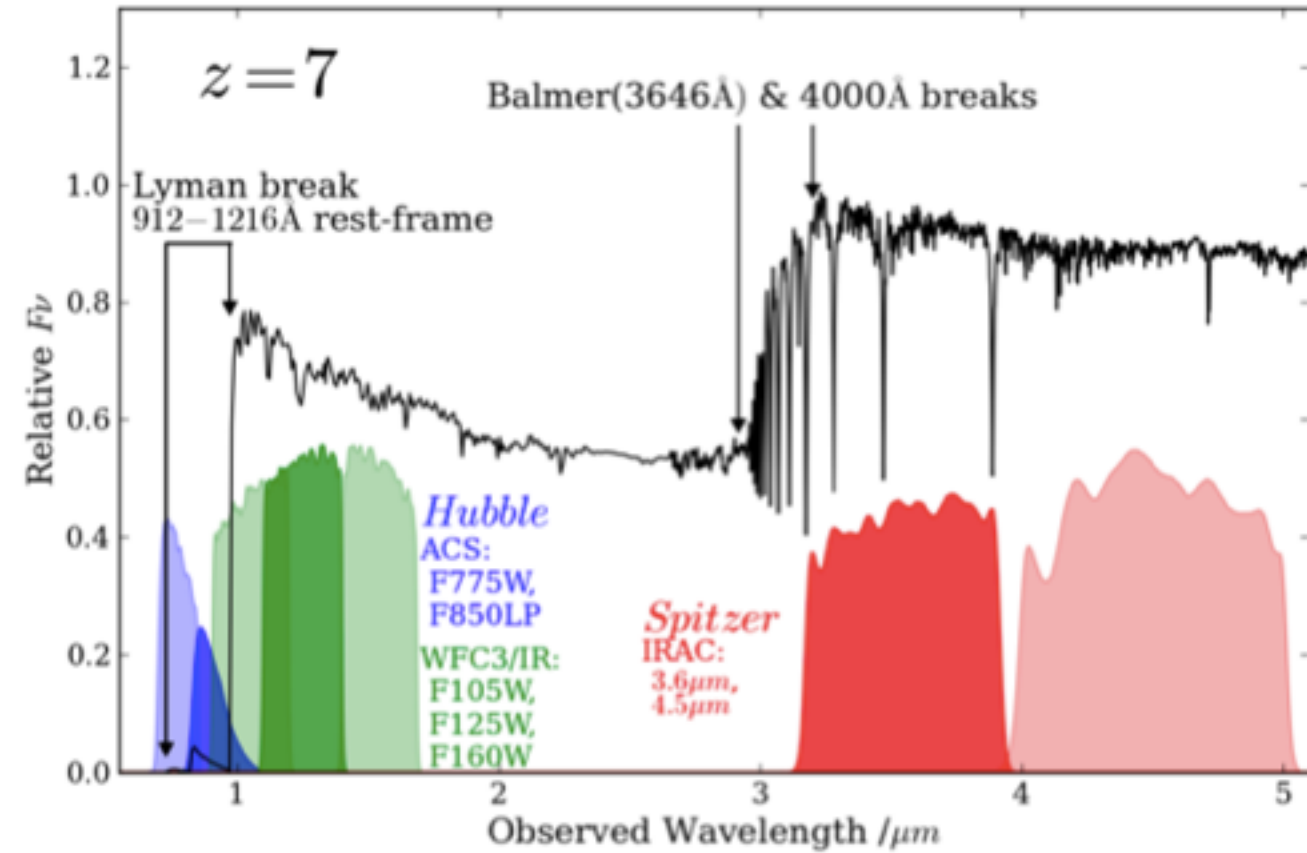
# Observations to select $4 < z < 8$ galaxies

## Observations requirements

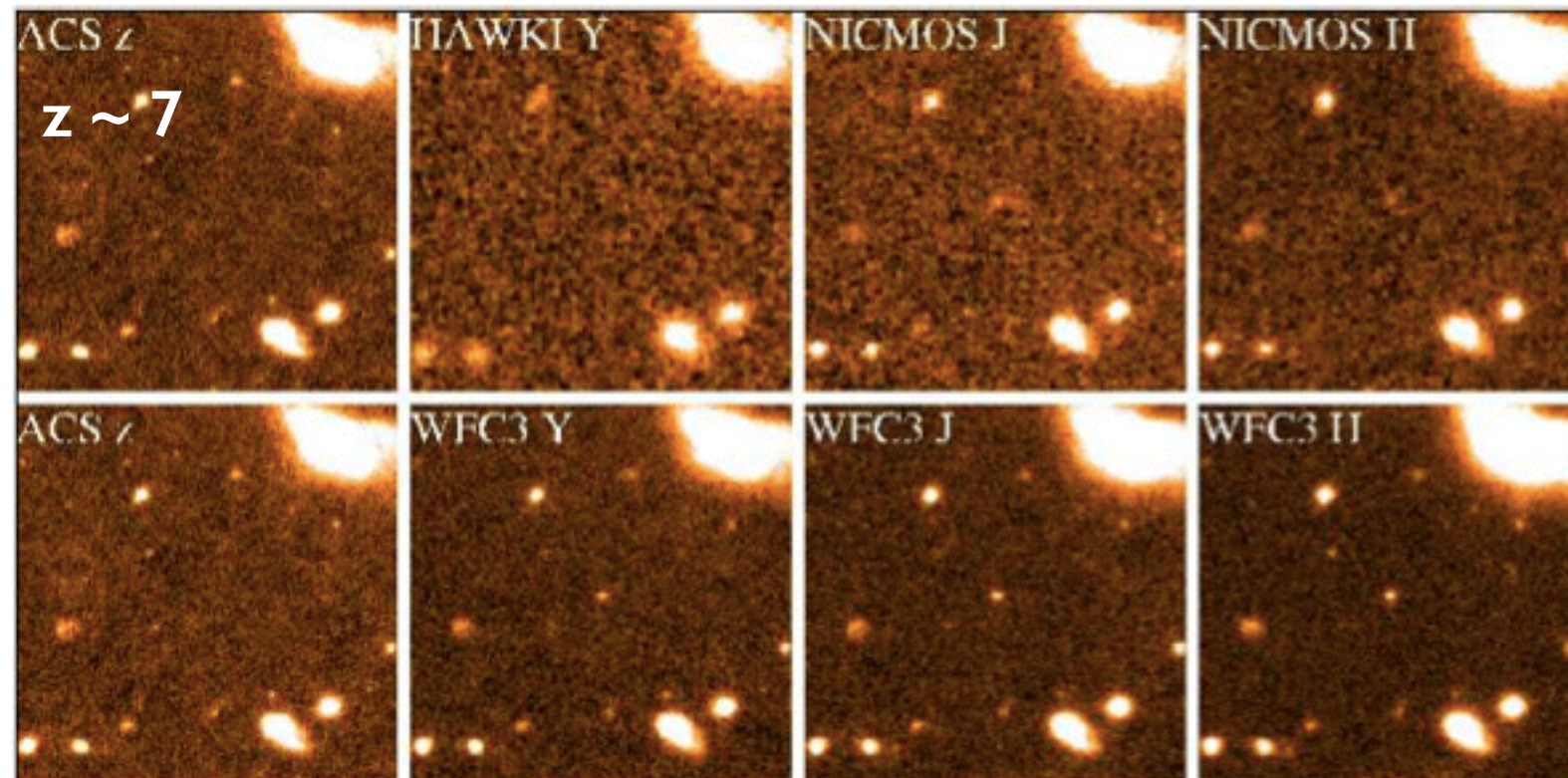
- multi-wavelength coverage
- deep imaging ( $\rightarrow$  limited to small areas)
- « large » area (massive gal. are rare)

## Selection with Lyman-Break Galaxies

- flux at  $\lambda < 912 \text{ \AA}$  absorbed by surrounding gas
- 90'-00': applied in optical  $\rightarrow z \sim 3-4-5$
- 2009: HST/WFC3 (+Spitzer/IRAC)  $\rightarrow z \sim 5-10$



Dunlop 2012



# Observations to select $4 < z < 8$ galaxies

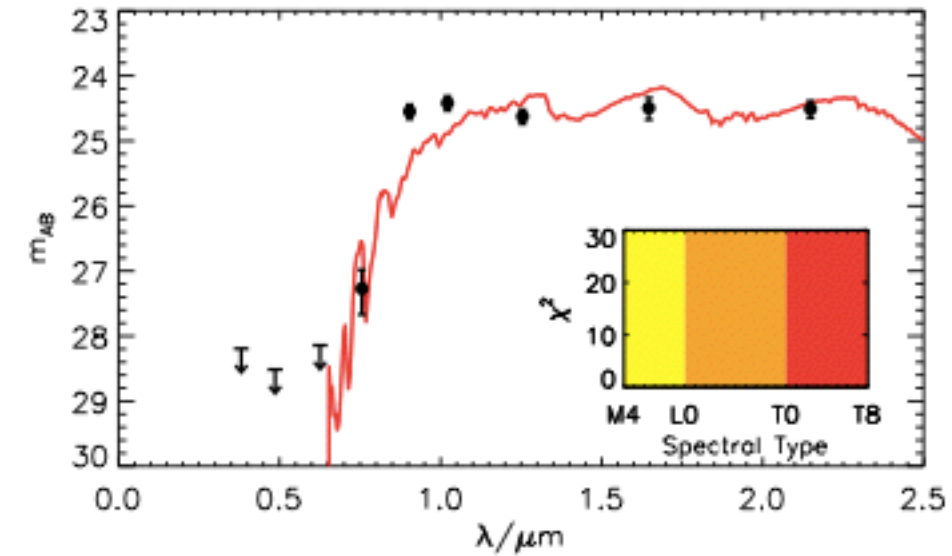
## Observations requirements

- multi-wavelength coverage
- deep imaging ( $\rightarrow$  limited to small areas)
- « large » area (massive gal. are rare)

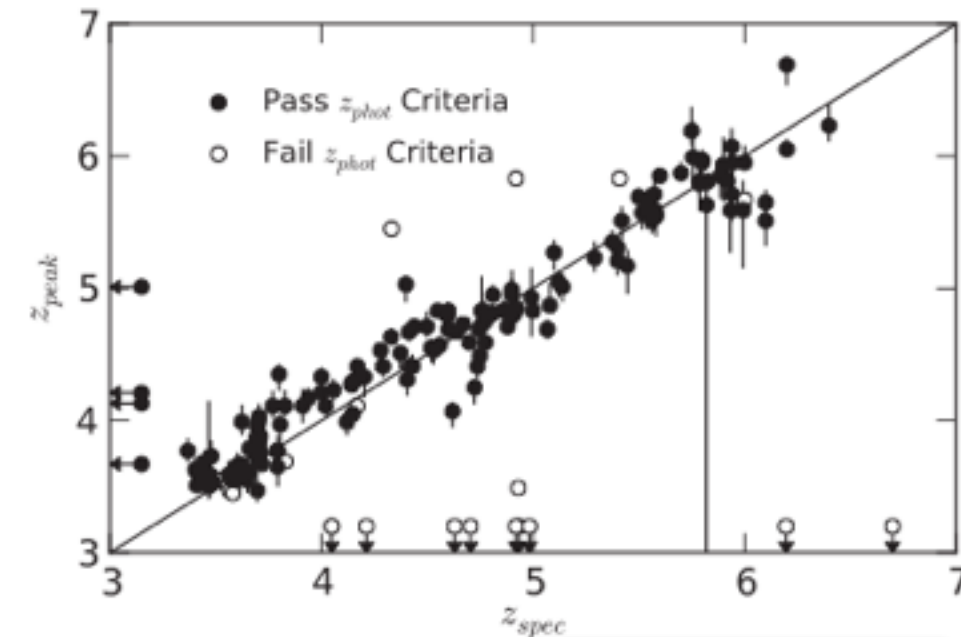
## Selection with Lyman-Break Galaxies

- flux at  $\lambda < 912 \text{ \AA}$  absorbed by surrounding gas
- 90'-00': applied in optical  $\rightarrow z \sim 3-4-5$
- 2009: HST/WFC3 (+Spitzer/IRAC)  $\rightarrow z \sim 5-10$

## Selection with photometric redshift



Bowler et al. 2015



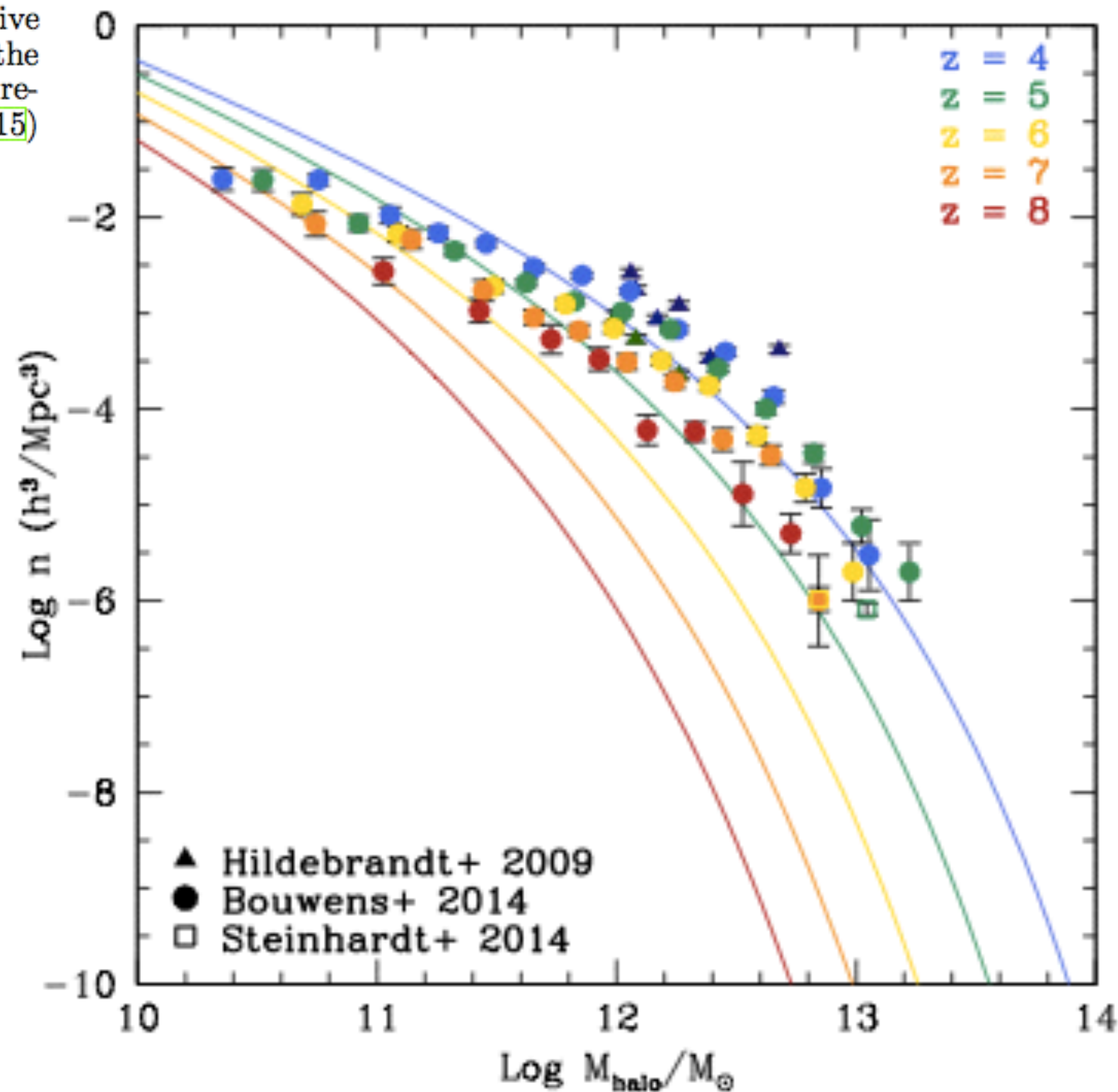
Duncan et al. 2014

# Observations to select $4 < z < 8$ galaxies

	Survey	Redshift range	Galaxy selection	Number of galaxies	Halo mass estimation
<b>Hildebrandt+09</b>	CFHTLS-deep (4 deg <sup>2</sup> )	$3 < z < 5$	Lyman-Break Galaxies	$\sim 8e4$	Clustering+HOD
<b>Steinhardt+14</b>	COSMOS (2 deg <sup>2</sup> )	$4 < z < 6$	photo-z	$\sim 3e3$	M(halo)/M(stellar)
<b>Duncan+14</b>	GOODS-S (160 arcmin <sup>2</sup> )	$4 < z < 7$	photo-z	$\sim 2e3$	
<b>Bouwens+15</b>	HST deep fields (1000 arcmin <sup>2</sup> )	$4 < z < 10$	Lyman-Break Galaxies (« enhanced »)	$\sim 1e4$	UV LF
<b>Bowler+15</b>	COSMOS+UDS ( $\sim 2$ deg <sup>2</sup> )	$5.5 < z < 6.5$	Lyman-Break Galaxies + photo-z	$\sim 3e2$	
<b>Finkelstein+15</b>	GOODS-N & S (320 arcmin <sup>2</sup> )	$4 < z < 7$	photo-z	$\sim 2e2$	Abundance matching

# « Data » versus model

compiled in Figure 1, showing the large and diverging disagreement between the theoretical and observational evolution of the halo mass function at high redshift. Specifically, we find that observational halo mass function estimates correspond to a higher number density of massive halos than should have been able to form through the rapid collapse and evolution of rare, highly-overdense regions (Fig. 1). The analysis of Finkelstein et al. (2015)



# From observations to halo mass

## Observations

(RA,DEC) + Multi-wavelength photometry

Halo mass and/or halo mass distribution

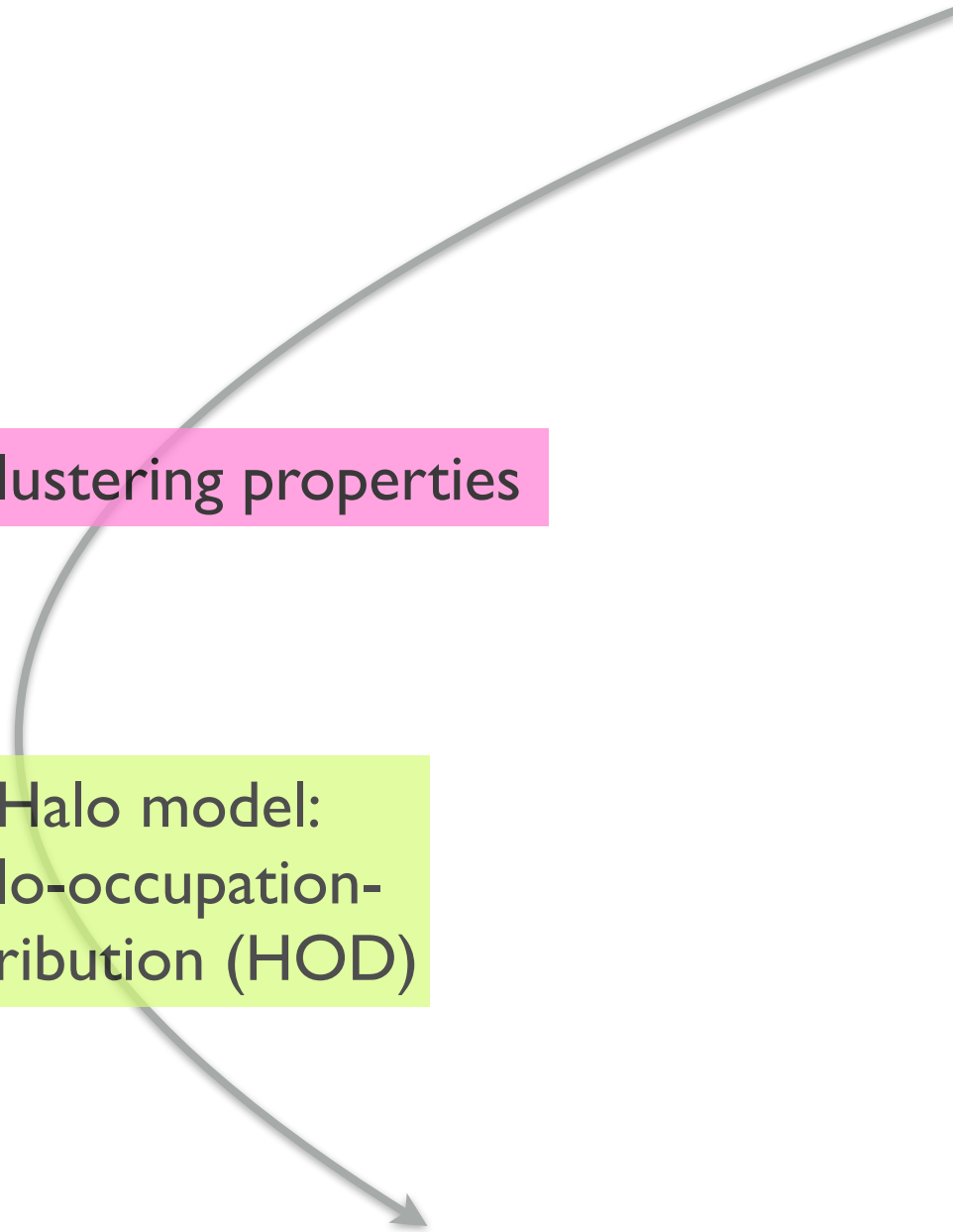
# From observations to halo mass

**Observations**  
(RA,DEC) + Multi-wavelength photometry

Clustering properties

Halo model:  
halo-occupation-  
distribution (HOD)

**Halo mass and/or halo mass distribution**



# From observations to halo mass

**Observations**  
(RA,DEC) + Multi-wavelength photometry

templates, scaling-relations

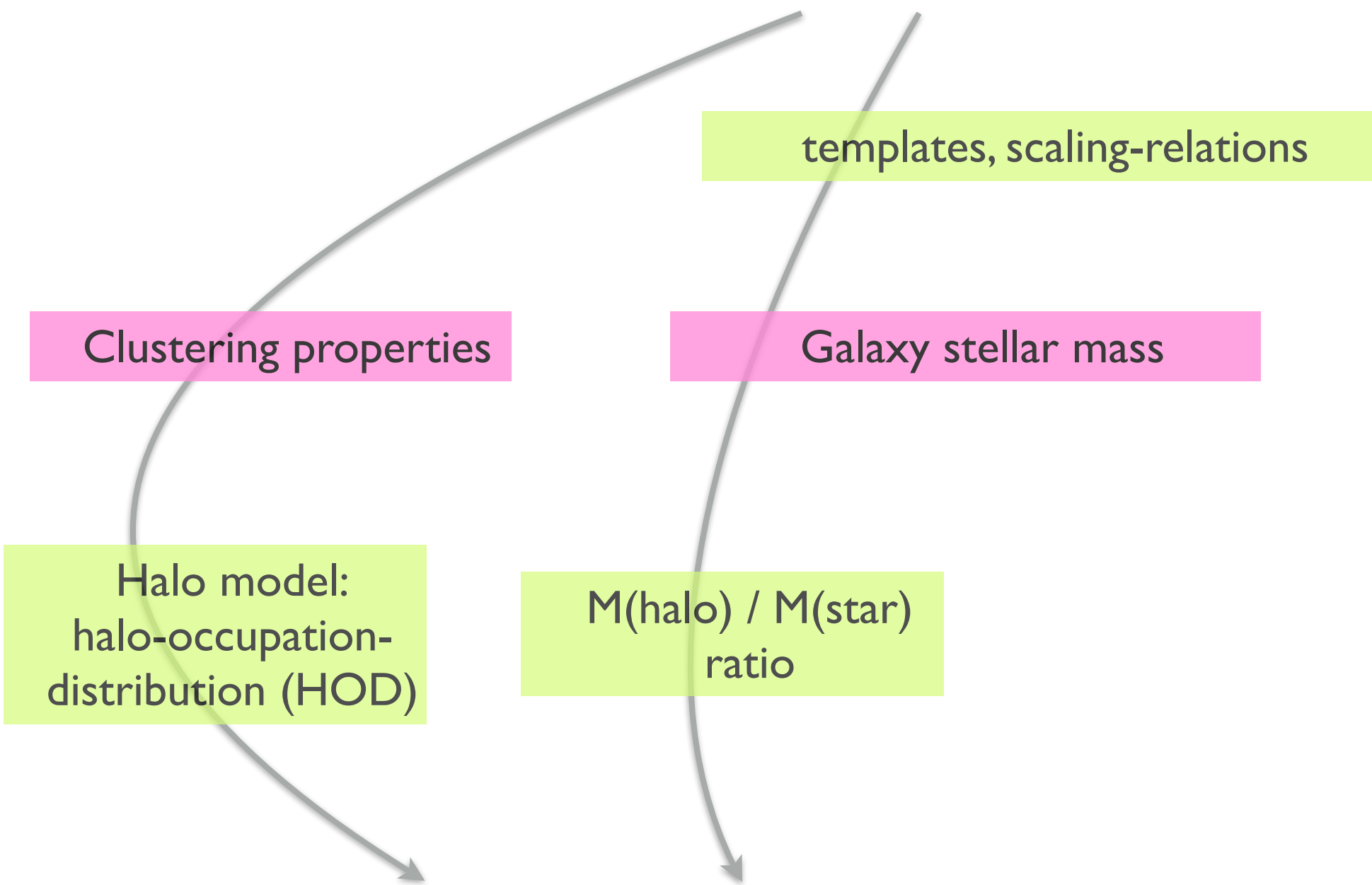
Clustering properties

Galaxy stellar mass

Halo model:  
halo-occupation-  
distribution (HOD)

$M(\text{halo}) / M(\text{star})$   
ratio

**Halo mass and/or halo mass distribution**



# From observations to halo mass

**Observations**  
(RA,DEC) + Multi-wavelength photometry

templates, scaling-relations

Clustering properties

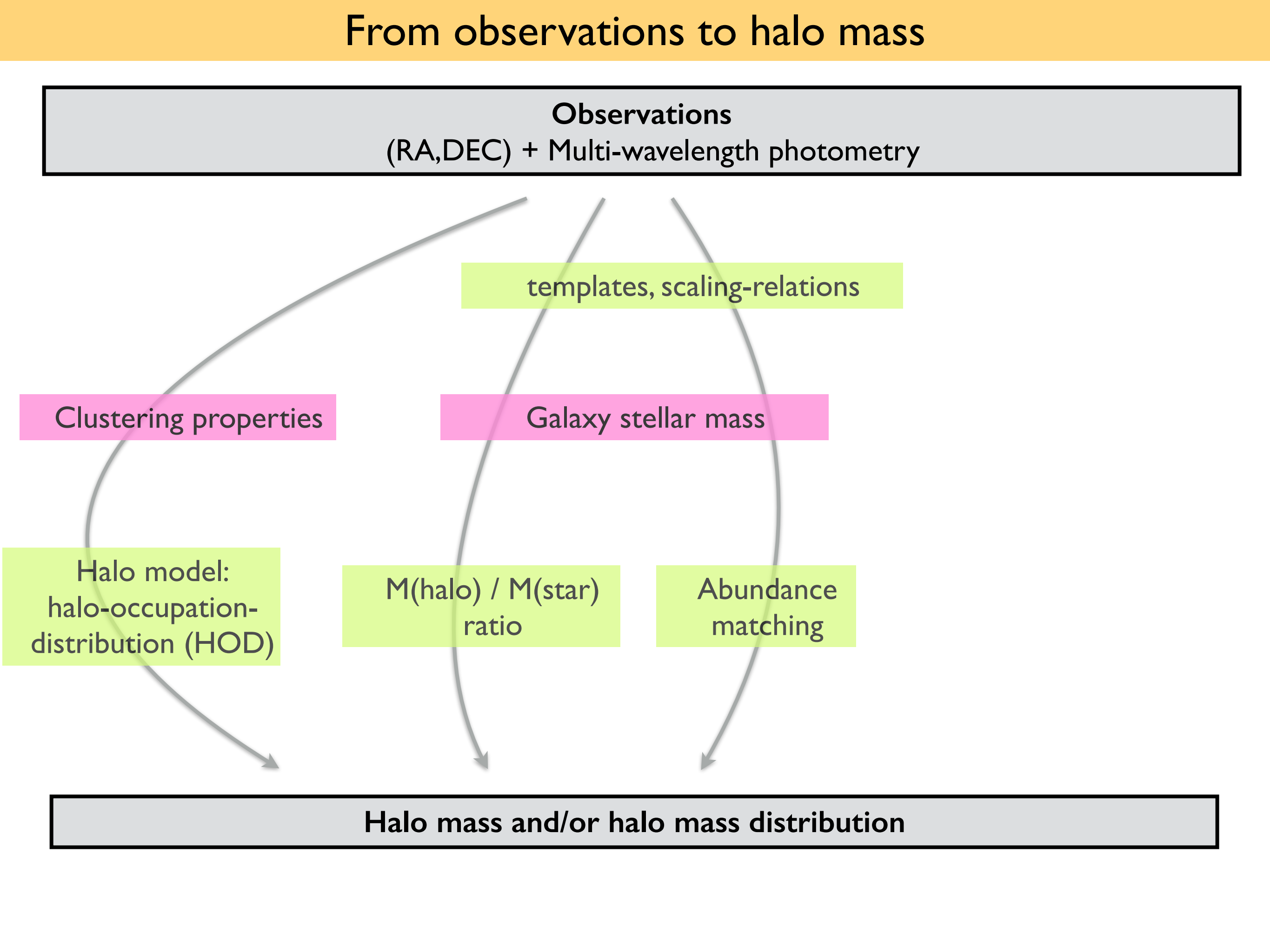
Galaxy stellar mass

Halo model:  
halo-occupation-  
distribution (HOD)

$M(\text{halo}) / M(\text{star})$   
ratio

Abundance  
matching

**Halo mass and/or halo mass distribution**



# From observations to halo mass

**Observations**  
(RA,DEC) + Multi-wavelength photometry

templates, scaling-relations

Clustering properties

Galaxy stellar mass

Rest-frame UV luminosity

Halo model:  
halo-occupation-  
distribution (HOD)

$M(\text{halo}) / M(\text{star})$   
ratio

Abundance  
matching

$M(\text{halo}) / L(\text{UV})$   
ratio

**Halo mass and/or halo mass distribution**

# From observations to halo mass

**Observations**  
(RA,DEC) + Multi-wavelength photometry

templates, scaling-relations ?

Clustering properties

Galaxy stellar mass

Rest-frame UV luminosity

Halo model:  
halo-occupation-  
distribution (HOD)

$M(\text{halo}) / M(\text{star})$   
ratio

Abundance  
matching

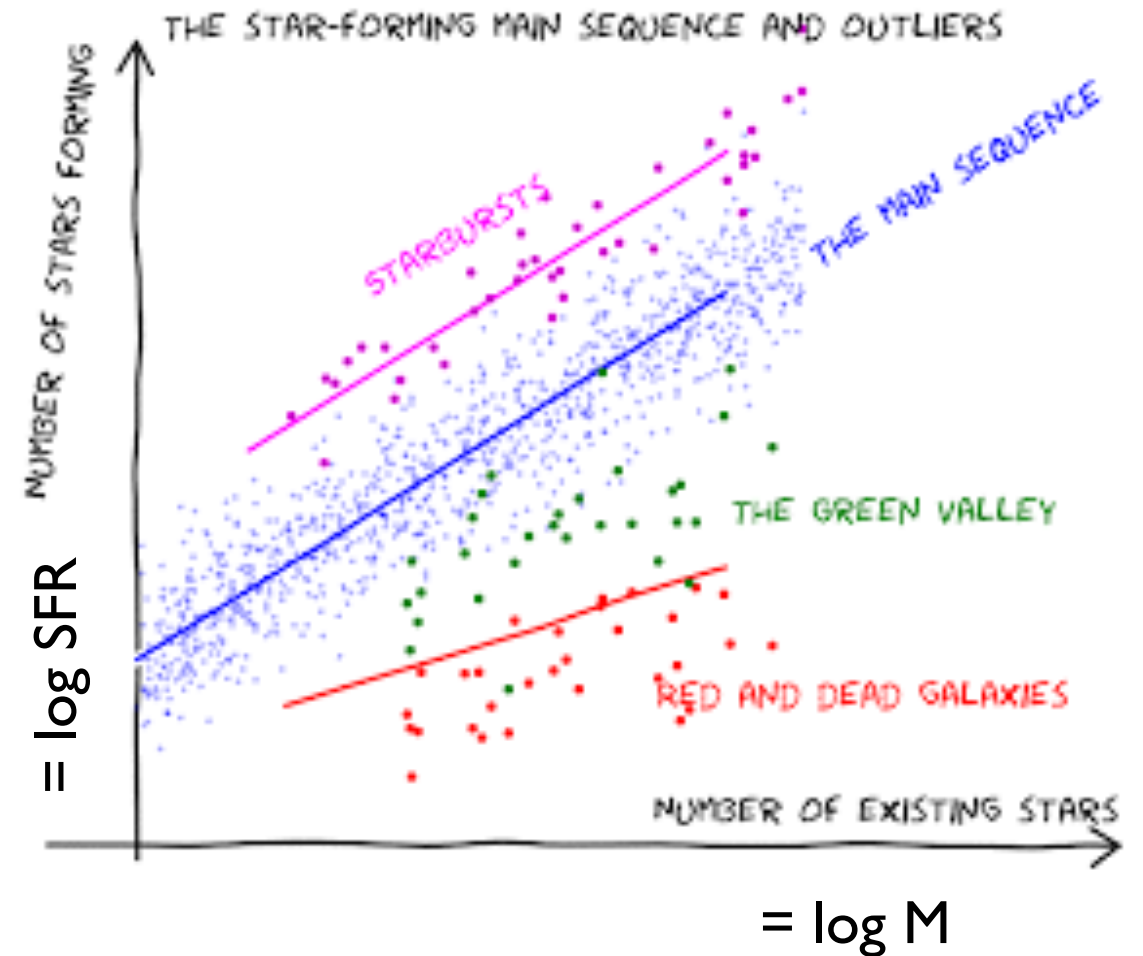
$M(\text{halo}) / L(\text{UV})$   
ratio

**Halo mass and/or halo mass distribution**

# Galaxy properties evolution ?

## Galaxy Main Sequence

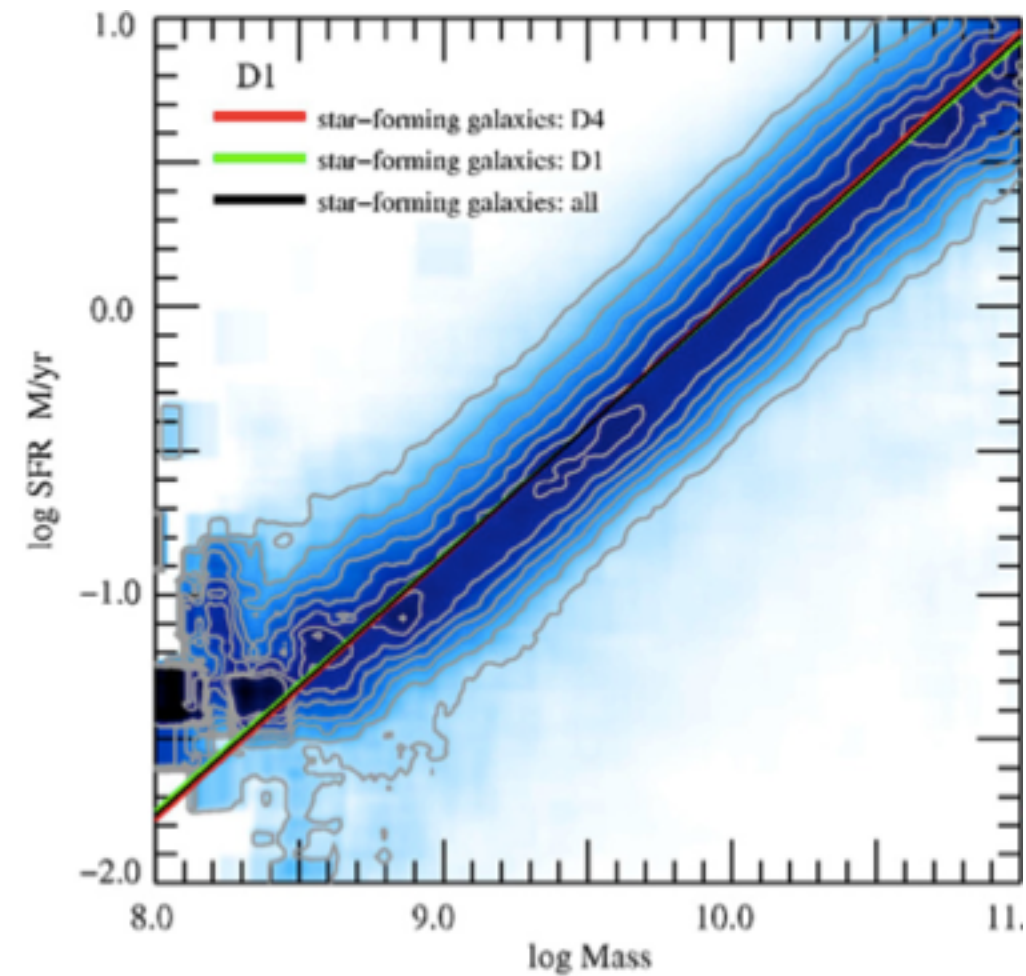
- for star-forming galaxies, the star-formation rate (SFR) is proportional to the galaxy stellar mass ( $\log M$ )



# Galaxy properties evolution ?

## Galaxy Main Sequence

- for star-forming galaxies, the star-formation rate (SFR) is proportional to the galaxy stellar mass ( $\log M$ )
- well-established at low-redshift

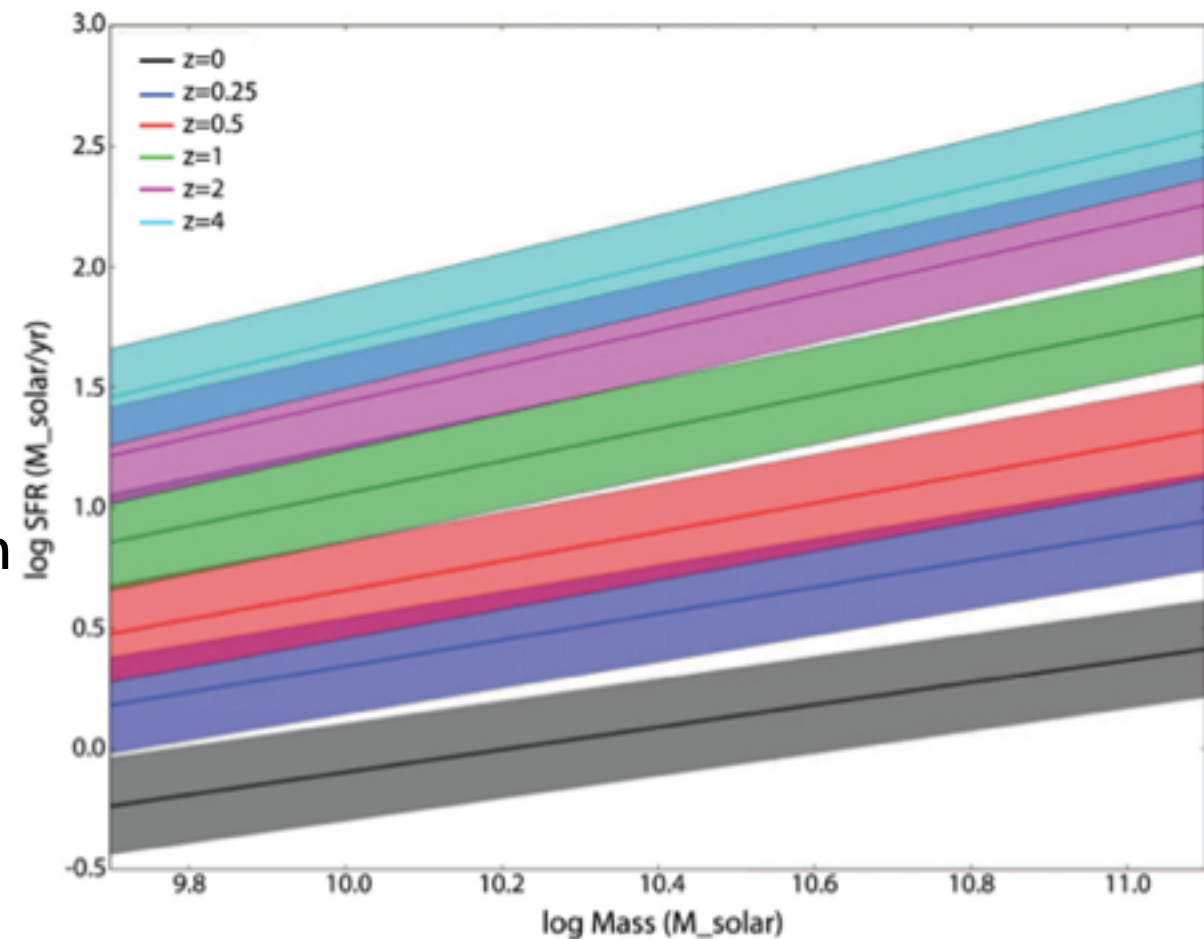


SDSS -  $z \sim 0.1$  Peng et al. 2010

# Galaxy properties evolution ?

## Galaxy Main Sequence

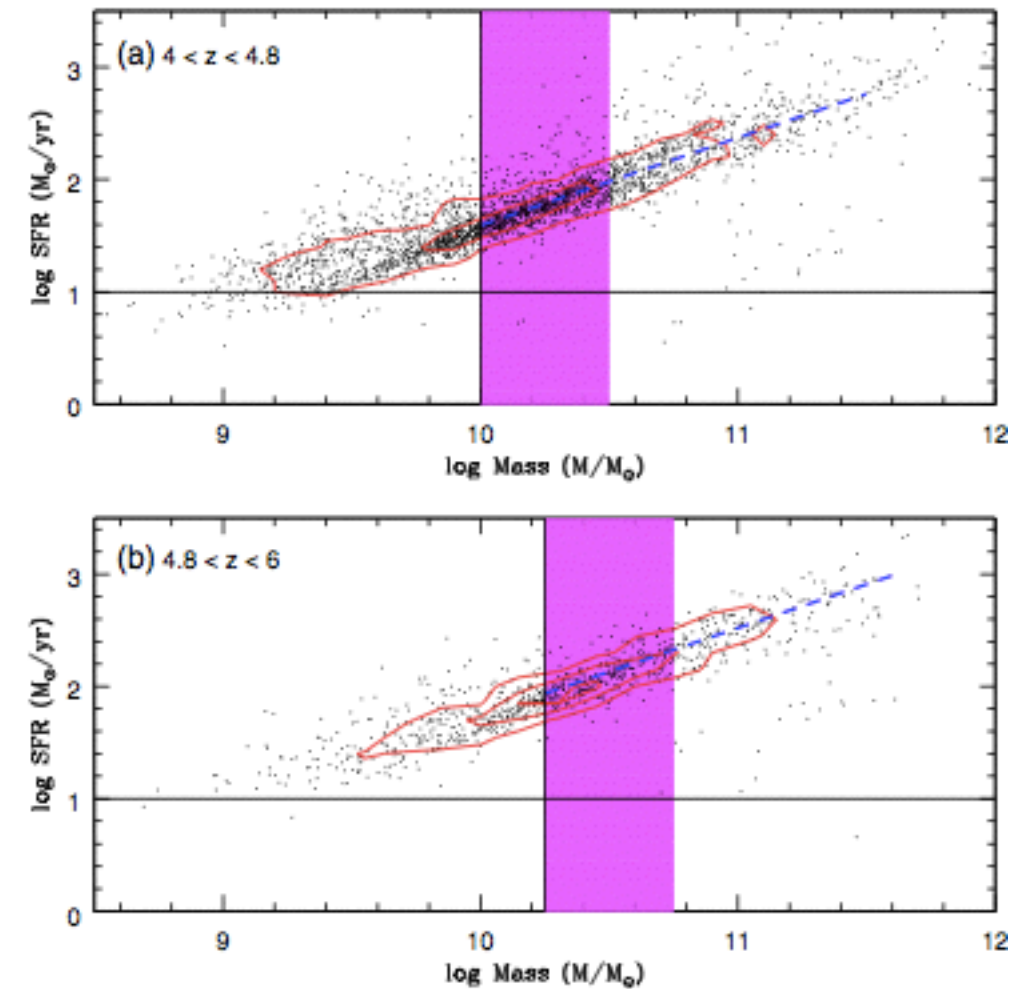
- for star-forming galaxies, the star-formation rate (SFR) is proportional to the galaxy stellar mass ( $\log M$ )
- well-established at low-redshift
- holds out to  $z=4$  (Speagle et al. 2014, compilation of 25 studies)



# Galaxy properties evolution ?

## Galaxy Main Sequence

- for star-forming galaxies, the star-formation rate (SFR) is proportional to the galaxy stellar mass ( $\log M$ )
- well-established at low-redshift
- holds out to  $z=4$  (Speagle et al. 2014, compilation of 25 studies)
- still valid at  $z=5$  and  $z=6$  (Steinhardt et al. 2014)



Steinhardt et al. 2014

# From observations to halo mass

**Observations**  
(RA,DEC) + Multi-wavelength photometry

templates, scaling-relations

Clustering properties

Galaxy stellar mass

Rest-frame UV luminosity

Halo model:  
halo-occupation-  
distribution (HOD)

$M(\text{halo}) / M(\text{star})$   
ratio

Abundance  
matching

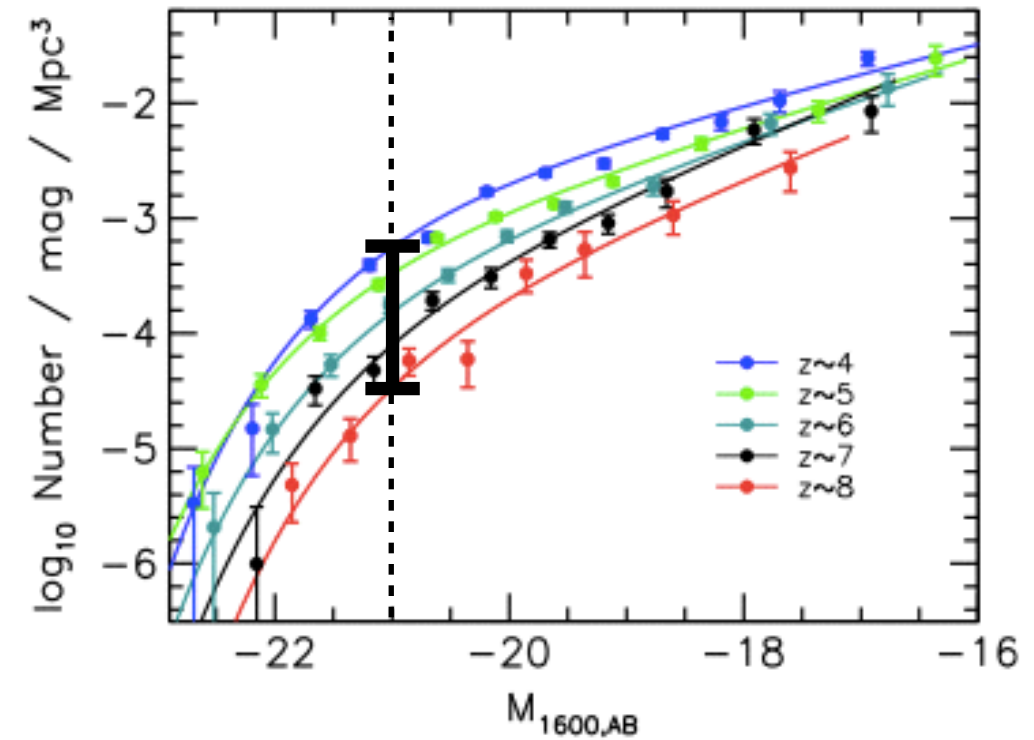
$M(\text{halo}) / L(\text{UV})$   
ratio ?

**Halo mass and/or halo mass distribution**

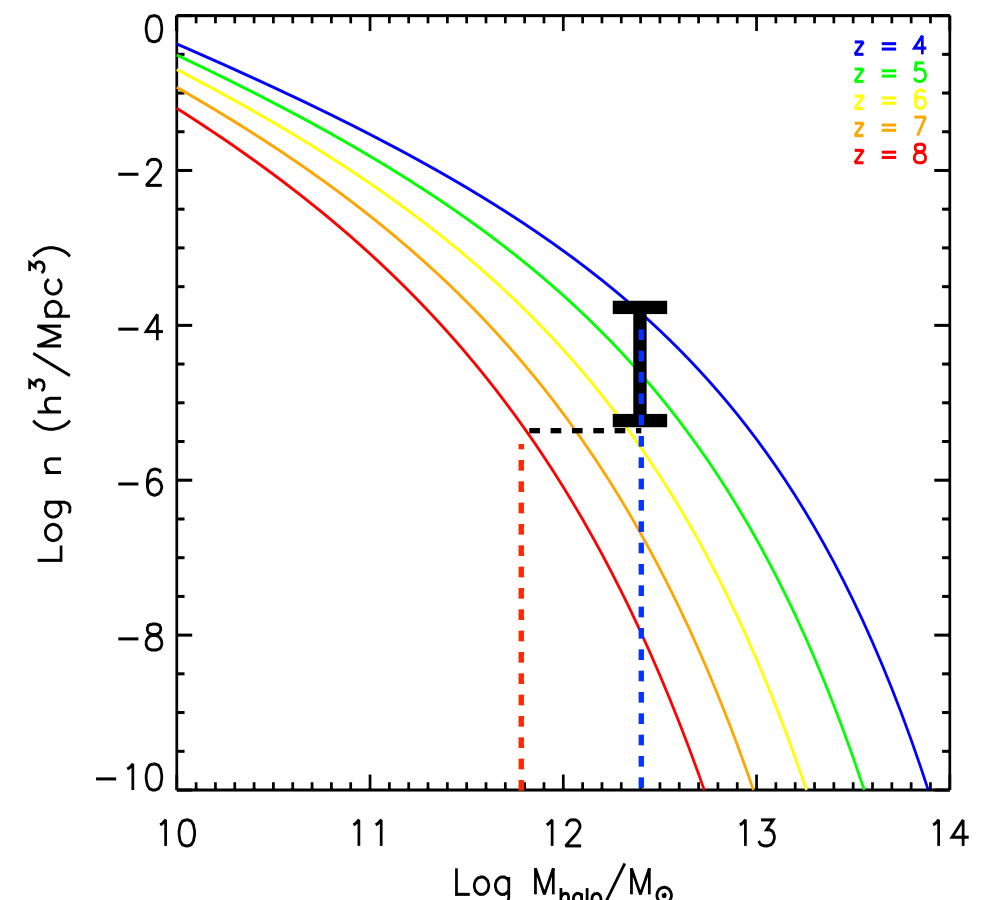
# M(halo) / UV LF ratio evolution ?

## Case of $M_{1600,AB}=21$ galaxies, $z=4 \rightarrow 8$

- $z=4$  :  $\log(M_{\text{halo}}/M_{\text{sun}})=12.4$
- evolution in number density in UV LF: 1.5dex
- implied evolution in  $M(\text{halo})$ : 0.8 dex



Bouwens et al. 2015



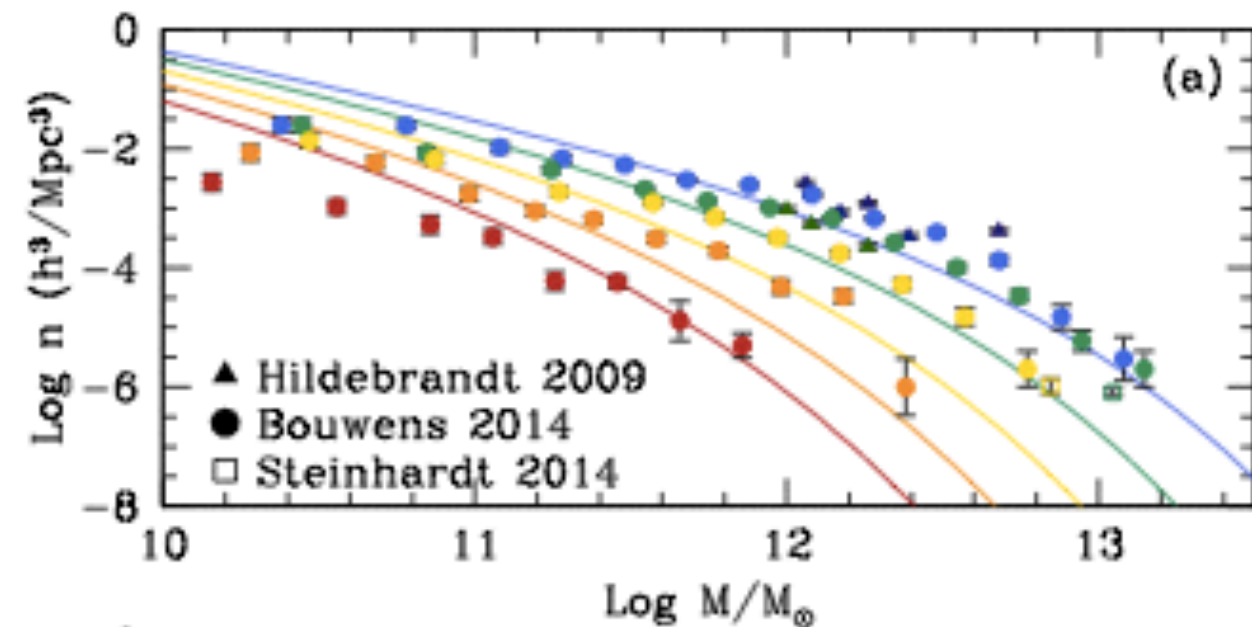
# M(halo) / UV LF ratio evolution ?

## Case of $M_{I600,AB}=21$ galaxies, $z=4 \rightarrow 8$

- $z=4$  :  $\log(M_{\text{halo}}/M_{\text{sun}})=12.4$
- evolution in number density in UV LF: 1.5dex
- implied evolution in  $M(\text{halo})$ : 0.8 dex

## Scenario #1

- all the stars in a galaxy formed in one short burst at  $z=8$
- ▶  $z=4$  galaxies would have 1 Gyr old, passive populations
- ▶ disagreement reported at  $z=6$



# M(halo) / UV LF ratio evolution ?

## Case of $M_{1600,AB}=21$ galaxies, $z=4 \rightarrow 8$

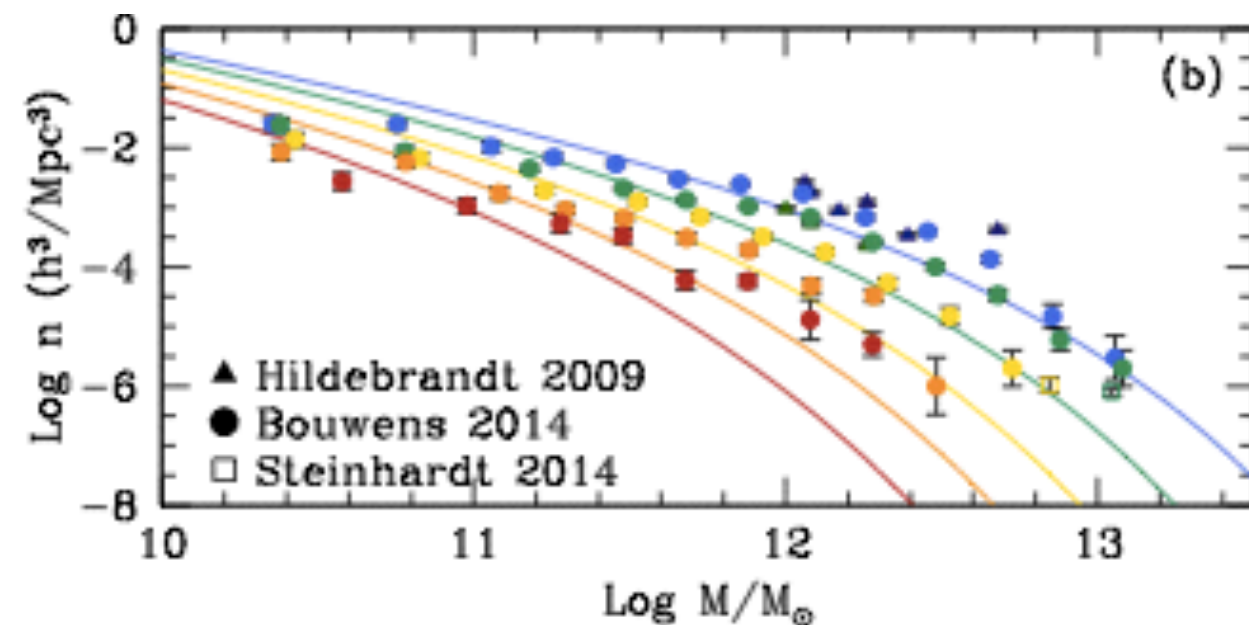
- $z=4$  :  $\log(M_{\text{halo}}/M_{\text{sun}})=12.4$
- evolution in number density in UV LF: 1.5dex
- implied evolution in  $M(\text{halo})$ : 0.8 dex

## Scenario #1

- all the stars in a galaxy formed in one short burst at  $z=8$
- ▶  $z=4$  galaxies would have 1 Gyr old, passive populations
- ▶ disagreement reported at  $z=6$

## Scenario #2

- one rapid burst at  $z=12$ , followed by evolution along the star-forming main sequence until observed at  $z=4-8$
- ▶ more realistic
- ▶ still insufficient to reconcile observation with theory



# M(halo) / UV LF ratio evolution ?

## Case of $M_{I600,AB}=21$ galaxies, $z=4 \rightarrow 8$

- $z=4$  :  $\log(M_{\text{halo}}/M_{\text{sun}})=12.4$
- evolution in number density in UV LF: 1.5dex
- implied evolution in  $M(\text{halo})$ : 0.8 dex

## Scenario #1

- all the stars in a galaxy formed in one short burst at  $z=8$
- ▶  $z=4$  galaxies would have 1 Gyr old, passive populations
- ▶ disagreement reported at  $z=6$

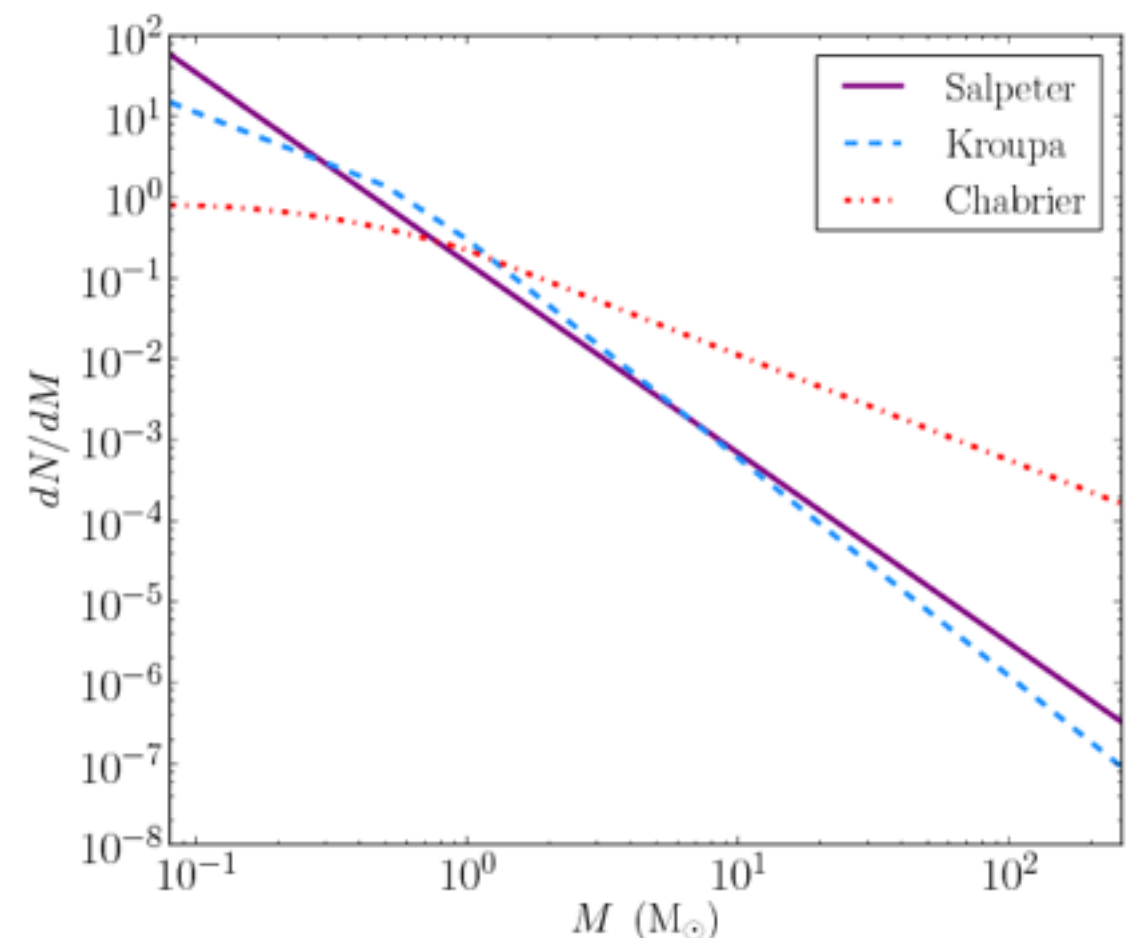
## Scenario #2

- one rapid burst at  $z=12$ , followed by evolution along the star-forming main sequence until observed at  $z=4-8$
- ▶ more realistic
- ▶ still insufficient to reconcile observation with theory

## Other possibility

- evolution of the IMF (Initial Mass Function)

Crosby et al. 2013



# From observations to halo mass

**Observations**  
(RA,DEC) + Multi-wavelength photometry

templates, scaling-relations

Clustering properties

Galaxy stellar mass

Rest-frame UV luminosity

Halo model:  
halo-occupation-  
distribution (HOD)

$M(\text{halo}) / M(\text{star})$   
ratio

Abundance  
matching

$M(\text{halo}) / L(\text{UV})$   
ratio

**Halo mass and/or halo mass distribution**

# M(halo) / M(star) ratio evolution ?

## Standard references

- $M(\text{star})/M(\text{baryon})=0.1$  of baryons ( $z < 1$ , Leauthaud+12)
- $M(\text{baryon})/M(\text{DM})=1/6$  (Planck 2015)

# M(halo) / M(star) ratio evolution ?

## Standard references

- $M(\text{star})/M(\text{baryon})=0.1$  of baryons ( $z < 1$ , Leauthaud+12)
- $M(\text{baryon})/M(\text{DM})=1/6$  (Planck 2015)

## Number density of galaxies as a function of haloes depends on:

- i) fraction of haloes containing a galaxy (Hildebrandt+09: 40% at  $z=5$ )
- ii) fraction of baryons converted into stars (Leauthaud+12: 10% at low- $z$ )
- iii) amount of time required after virialization for those stars to have formed

# M(halo) / M(star) ratio evolution ?

## Standard references

- $M(\text{star})/M(\text{baryon})=0.1$  of baryons ( $z < 1$ , Leauthaud+12)
- $M(\text{baryon})/M(\text{DM})=1/6$  (Planck 2015)

## Number density of galaxies as a function of haloes depends on:

- i) fraction of haloes containing a galaxy (Hildebrandt+09: 40% at  $z=5$ )
- ii) fraction of baryons converted into stars (Leauthaud+12: 10% at low- $z$ )
- iii) amount of time required after virialization for those stars to have formed

## Requirements to have $2 \cdot 10^{-5} \text{Mpc}^{-3}$ for $M_* = 10^{11} M_\odot$ at $z=5.5$

- ▶ implausible physics:
  - ▶ all baryons instantaneously turned into stars
  - ▶ halo mass  $< 10^{12} M_\odot$

Halo Occ.	Baryon Frac	SF Time	$M_{\text{halo}}/M_\odot$	$z_{\text{form}}$
10%	100%	Instant	$5 \times 10^{11}$	5.5
100%	30%	Instant	$2 \times 10^{12}$	5.5
100%	100%	150 Myr	$5 \times 10^{11}$	6.4
100%	10%	(-1.1 Gyr)	$5 \times 10^{12}$	3.0

TABLE 1

VARIOUS COMBINATIONS OF PARAMETERS PRODUCING THE OBSERVED NUMBER DENSITY OF  $10^{11} M_\odot$  GALAXIES AT  $z = 5.5$ .

# arxiv evolution... Bouwens et al. 2015

Comments: 50 pages, 28 figures, 10 tables, updated in response to comments by the referee

Subjects: **Cosmology and Nongalactic Astrophysics (astro-ph.CO)**; Astrophysics of Galaxies (astro-ph.GA)

Cite as: [arXiv:1403.4295](https://arxiv.org/abs/1403.4295) [astro-ph.CO]

(or [arXiv:1403.4295v3](https://arxiv.org/abs/1403.4295v3) [astro-ph.CO] for this version)

## Submission history

From: Rychard J. Bouwens [[view email](#)]

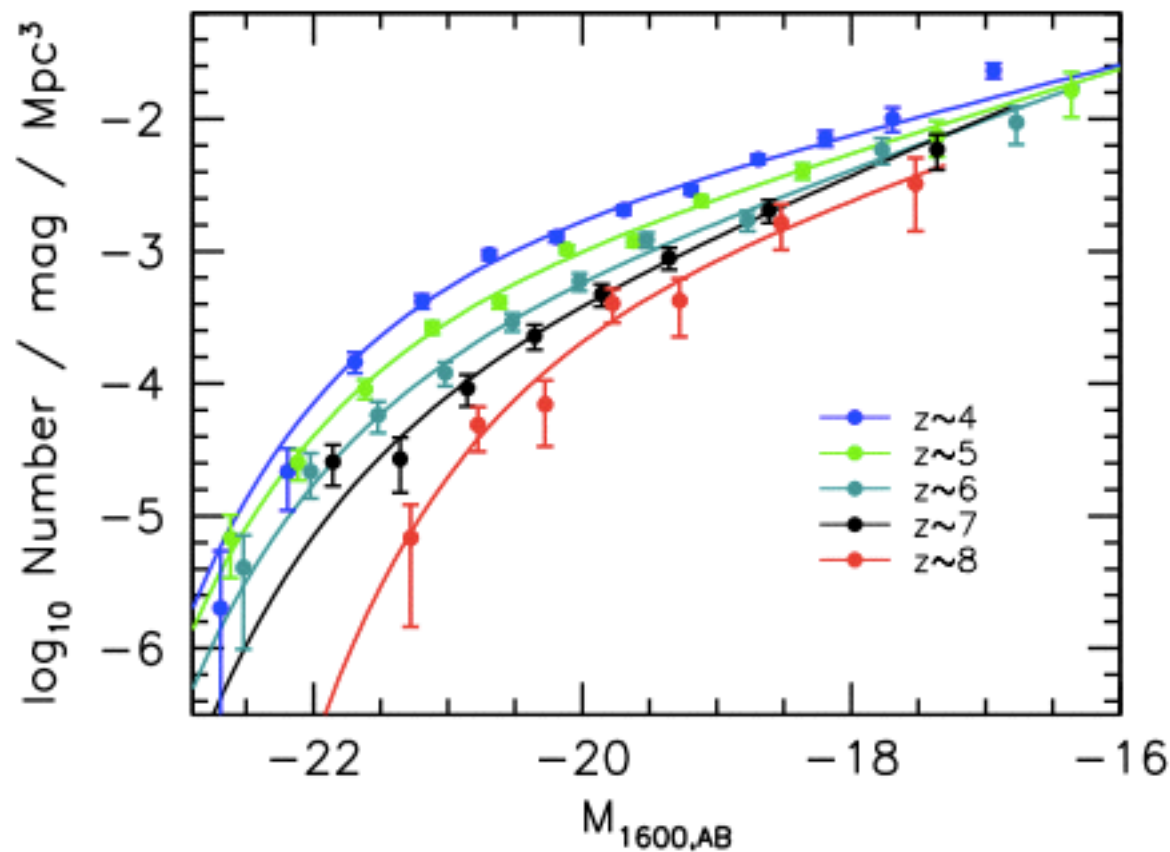
[v1] Mon, 17 Mar 2014 22:35:11 GMT (1011kb)

[v2] Tue, 29 Apr 2014 13:56:13 GMT (1011kb)

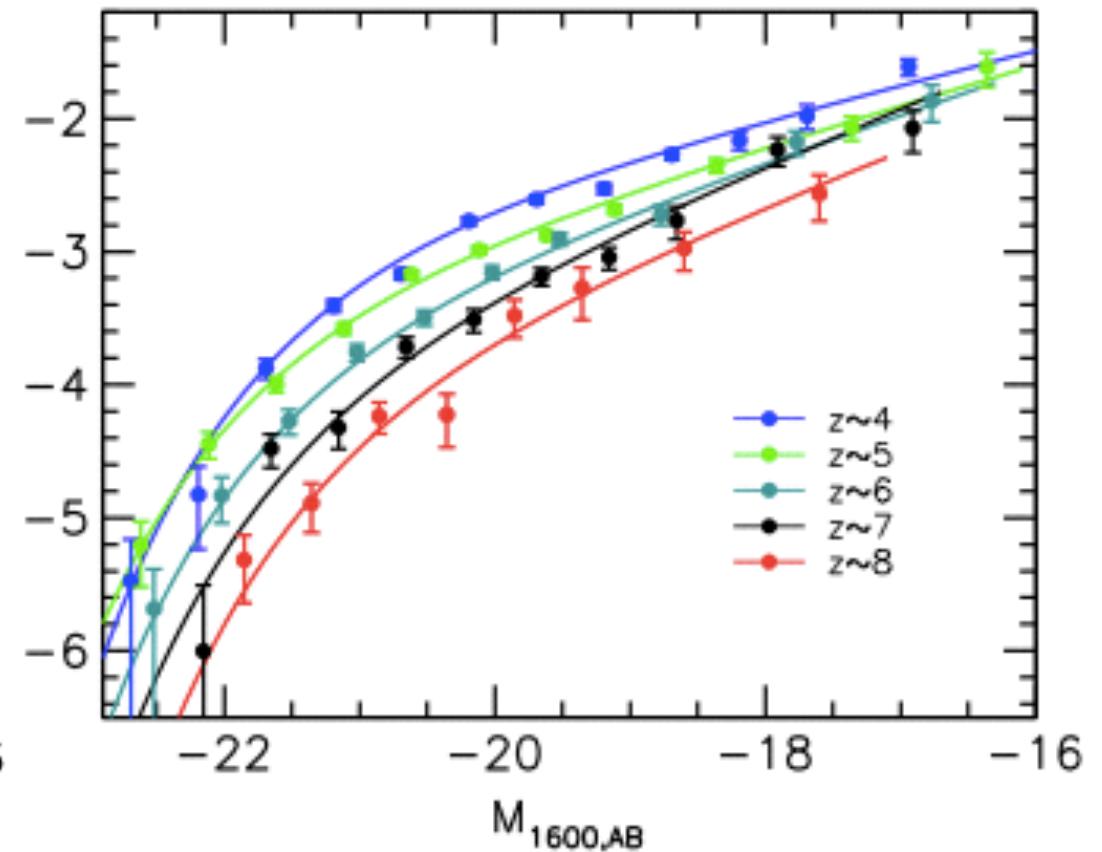
[v3] Mon, 3 Nov 2014 20:55:59 GMT (1023kb)

[v4] Thu, 22 Jan 2015 19:17:11 GMT (1041kb)

[v1]



[v3]



# What about semi-analytical models?

## Principle

- use semi-analytical prescriptions for connecting the properties of massive galaxies to their halo (info drawn from low-z relationships)
- ▶ cannot produce massive galaxies at  $z > 4$ , with « reasonable properties »

## Millenium simulation (Springel+05)

- can produce  $M_* = 10^{11} M_\odot$  at  $z=6$ , but with  $M(\text{halo}) = 10^{11.3} M_\odot$
- ▶ would require the baryons to cluster in advance of much of the DM
- ▶ would imply nearly all baryons to have ended up in stars by  $z=6$
- ▶ in conflict with observations (Hildebrandt+09, Finkelstein+15)

## Illustris simulation (Vogelsberger+14)

- baryonic relationships that avoids unphysical extrapolations
- luminosity and stellar mass functions that look similar to the halo mass function
- ▶ number densities consistent with observations out to  $M_* = 10^{10} M_\odot$
- ▶ but too few galaxies with  $M_* > 10^{10.5} M_\odot$ , in conflict with observations

# Conclusion

## Failed template fitting

- re-consider the assumption that templates derived from low- $z$  galaxies can be used at  $z=6$
- ▶ one likely explanation is a top-heavier IMF at high- $z$
- ▶ can be tested with supernovae rates; then with JWST

## Early star formation

- allow main sequence star formation much early than the initial collapse of haloes
- ▶ difficult constrain from low- $z$  observations
- ▶ problem of cooling to form small stars at low metallicities

## New clustering physics

- haloes collapse earlier than allowed by current models
- ▶ warm dark matter would suppress the  $z\sim 6$  halo mass function rather than enhance it
- ▶ dark energy with  $w > -1$  could enhance early structure formation, though Planck observations create considerable tension with the  $w > -0.95$  required to solve this problem

## Better observations are needed

- high-mass objects at high- $z$  bring crucial constraints
- ▶ need for wide area surveys ( $> 1$  degree)



# Hildebrandt+09 - Halo Occupation Distribution (HOD)

## Clustering analysis

- possible because « large » area of the CFHTLS-deep
- galaxy density  $n_g$
- correlation length  $r_0$
- slope of the correlation function  $\gamma$
- bias  $b$

$$w(\theta) = A \theta^{-\delta} \quad \xi(r) = (r/r_0)^{-\gamma}$$

## Halo model

This excess on small scales is interpreted in both studies as being due to the contribution from a 1-halo term of galaxy pairs residing in the same halos. We apply the halo model by Hamana et al. (2004) to our data to have a direct comparison with the  $z = 4$  results from Ouchi et al. (2005) who use the same model.

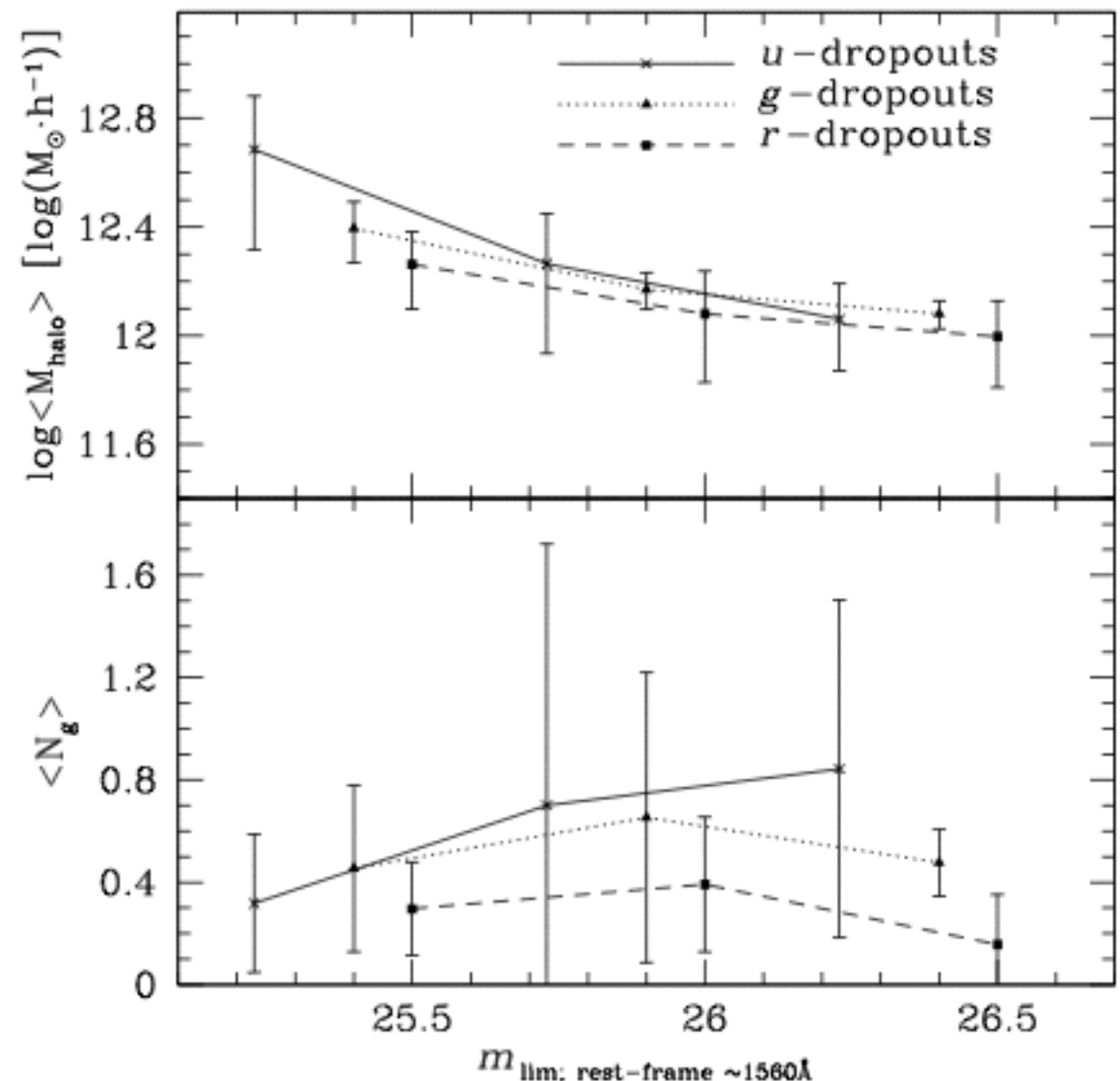
In this model the angular correlation function of LBGs is calculated from the CDM angular correlation function by applying the following halo-occupation-distribution (HOD) for single galaxies:

$$N_g(M) = \begin{cases} (M/M_1)^\alpha & \text{for } M > M_{\min} \\ 0 & \text{for } M < M_{\min} \end{cases} \quad (7)$$

and the following HOD for pairs of galaxies:

$$\langle N_g(N_g - 1) \rangle(M) = \begin{cases} N_g^2(M) & \text{if } N_g(M) > 1 \\ N_g^2(M) \log[4N_g(M)] / \log 4 & \text{if } 1 > N_g(M) > 0.25, \\ 0 & \text{otherwise} \end{cases} \quad (8)$$

with  $N_g(M)$  being the number of galaxies in a halo of mass  $M$ ,  $\langle N_g(N_g - 1) \rangle(M)$  being the number of galaxy pairs in a halo of mass  $M$ , and  $M_{\min}$ ,  $M_1$ , and  $\alpha$  being the parameters of the model. Furthermore, we calculate the number density of LBGs from this model as described in Hamana et al. (2004).



# Finkelstein+15 - Abundance matching

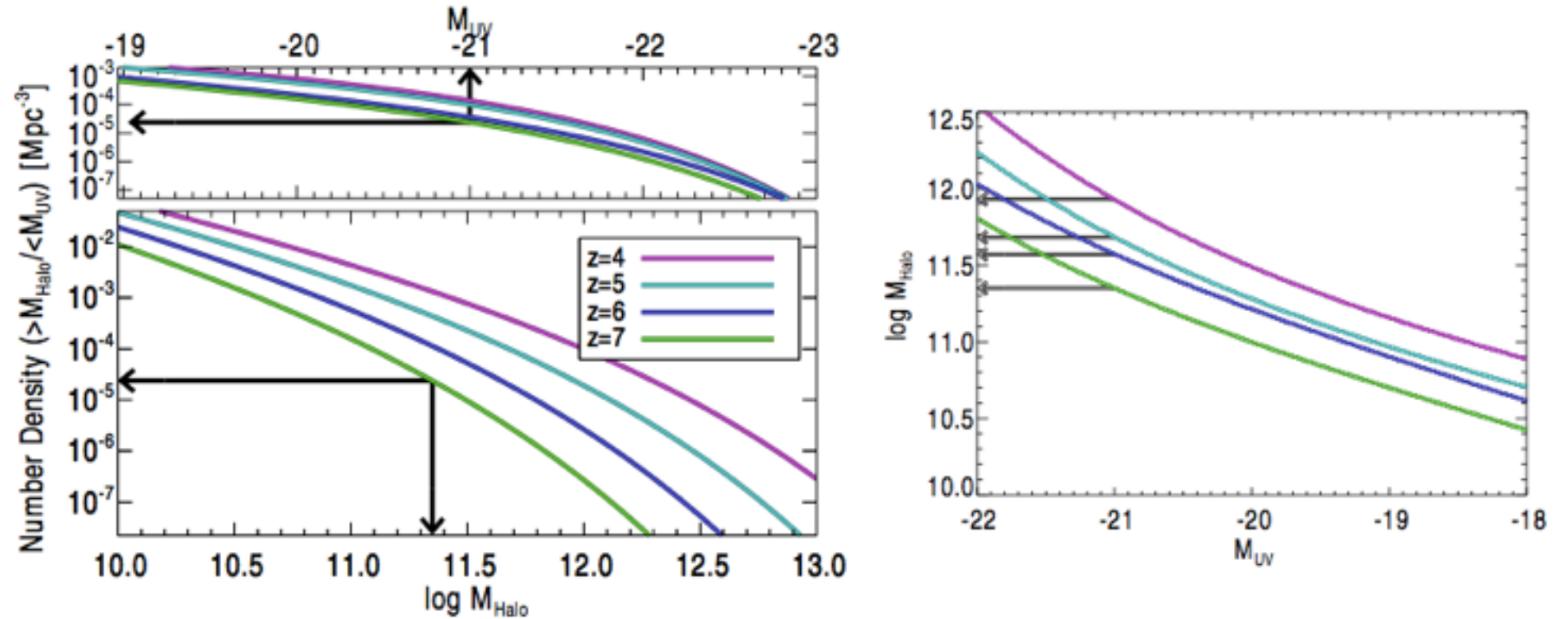


FIG. 3.— Top left: The cumulative luminosity function at  $z = 4, 5, 6,$  and  $7$ . Bottom Left: Cumulative halo mass functions at  $z = 4, 5, 6,$  and  $7$ , derived by volume-averaging the Bolshoi snapshot mass functions over the same redshift ranges as those defining our galaxy samples. The arrows show our results from abundance matching at  $z = 7$ , where galaxies with  $M_{1500} < -21$ , which have  $n(M_{\text{UV}} < -21) = 2.5 \times 10^{-5} \text{ Mpc}^{-3}$ , have halo masses of  $\log(M_h/M_\odot) = 11.35$ . Right: Relation between observed UV absolute magnitude and abundance-matching-derived halo mass at our redshifts of interest. The arrows denote the halo masses at our magnitude of interest of  $M_{\text{UV}} = -21$ .

- by construction, the UV LF and halo mass function are in agreement
- inconsistency pushed into the stellar to halo mass ratio

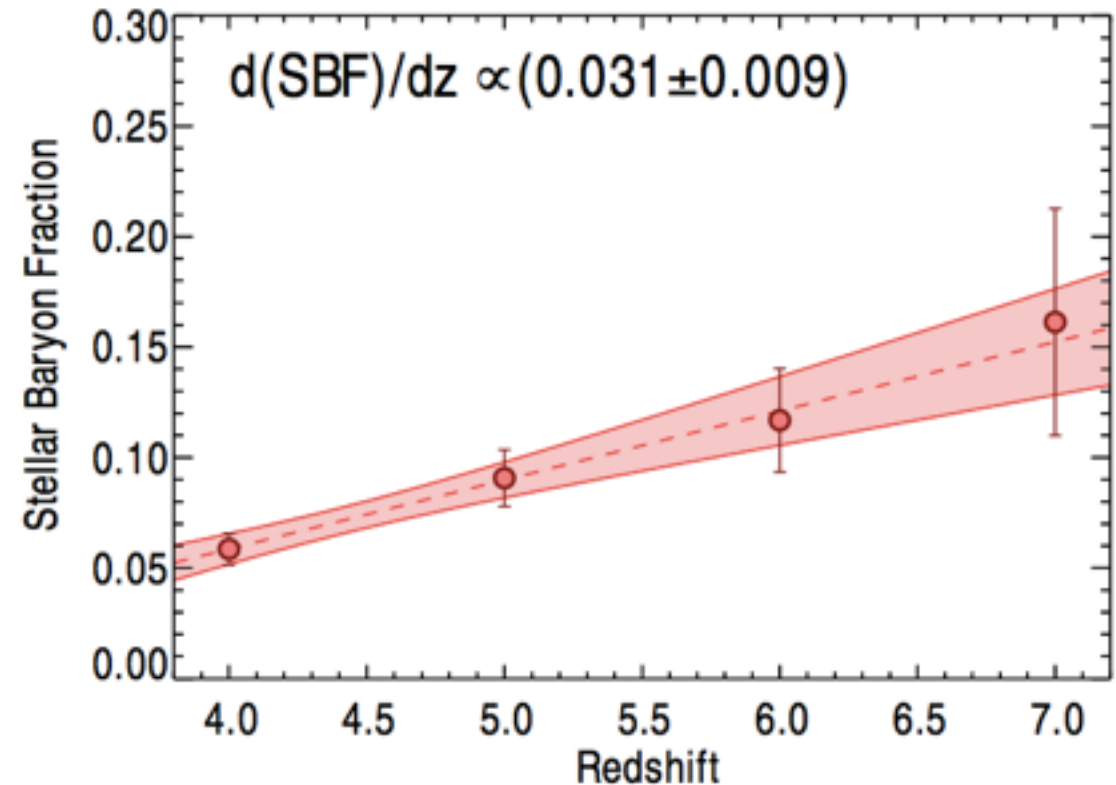


FIG. 4.— The stellar baryon fraction (SBF) in bright ( $M_{\text{UV}} = -21$ ) galaxies from  $z = 4$  to  $7$ . We define the SBF as the stellar to halo mass ratio in units of the cosmic baryon mass fraction  $\Omega_b/\Omega_m$ . We find that the SBF increases with increasing redshift, which may be responsible for the apparent lack of evolution in the characteristic magnitude  $M_{\text{UV}}^*$  observed over this redshift range.

# Bouwens+15 - Building the $4 < z < 8$ UV LF

Bouwens2015.pdf (page 15 sur 49)

15

**Bouwens2015.pdf**

- 1. INTRODUCTION
- 2. OBSERVATIONAL DATA SETS
- ▼ 3. SAMPLE SELECTION
  - ▶ 3.1. Photometry
  - ▶ 3.2. Source Selection
  - 3.3. Selection Results
  - 3.4. Comparisons with Previous  $z \sim 4-10$  Samples
  - ▼ 3.5. Contamination
    - 3.5.1. Stars
    - 3.5.2. Transient Sources or Supernovae
    - 3.5.3. Lower-redshift Galaxies
    - 3.5.4. Extreme Emission Line Galaxies
    - 3.5.5. Establishing the Contamination from Low-reds...
    - 3.5.6. Spurious Sources
    - 3.5.7. Summary
- ▼ 4. LUMINOSITY FUNCTION RESULTS
  - 4.1. SWML Determinations
  - 4.2. Schechter Function Fit Results
  - 4.3. Comparison against Previous Results
  - 4.4. Non-Schechter-like Shape of the LF at  $z \sim 4-10$
  - 4.5. Field-to-field Variations
  - 4.6.  $z \sim 4-10$  LF Results
- ▼ 5. DISCUSSION
  - 5.1. Empirical Fitting Formula for Interpolating and Extr...
  - 5.2. Faint-end Slope Evolution
  - 5.3. SFR Evolution in Individual Galaxies
  - 5.4. Luminosity and Star Formation Rate Densities
  - ▶ 5.5. Comparison with Theoretical Models
- 6. SUMMARY
- ▶ APPENDIX A OTHER DETAILED INFORMATION ON THE OBSE...
- ▶ APPENDIX B INITIAL PHOTOMETRIC SET OF  $z \sim 4-10$
- ▶ APPENDIX C SURFACE DENSITY OF  $z \sim 4-10$
- ▶ APPENDIX D ENSURING THE MODEL SIZE DISTRIBUTION OF...
- ▶ APPENDIX E TESTING OUR  $z \sim 4-10$
- ▶ APPENDIX F COMPARISONS AGAINST PREVIOUS  $z \sim 4-10$
- ▶ APPENDIX G ROBUSTNESS OF OUR CONSTRAINTS ON THE B...
- ▶ APPENDIX H COMPARISONS AGAINST THE TOTAL MAGNITU...
- ▶ APPENDIX I BOUWENS ET AL. (2008) CONDITIONAL LF MODEL
- REFERENCES

THE ASTROPHYSICAL JOURNAL, 803:34 (49pp), 2015 April 10

BOUWENS ET AL.

would expect contamination from stellar sources to be somewhat limited. Bouwens et al. (2006) found the SExtractor stellerity parameter to be very effective in distinguishing point sources from extended sources, for sources with sufficiently high S/N (i.e.,  $>10$ ).

Near the detection limit of our samples, a small level of contamination is expected, given that we no longer attempt to remove point sources at such low S/Ns. We estimated this contamination by deriving the number counts for all point-like sources in the CANDELS fields (stellerity  $>0.9$ ) that would satisfy our selection criteria if placed near the selection limit of surveys. We identified  $\sim 25$  stars over the magnitude range  $21 < H_{160,AB} < 26$  per CANDELS field that could contaminate our  $z \sim 4-10$  selections, with no especially significant increase in the surface density of such sources from  $H_{160,AB} \sim 21$  to  $H_{160,AB} \sim 26$  (similar to that found by Pirzkal et al. 2009). This is equivalent to a surface density of  $\sim 0.04$  arcmin $^{-2}$  mag $^{-1}$ , which is within a factor of two of the surface density of low-mass stars (M4 and later) found by Pirzkal et al. (2009) and Holwerda et al. (2014b), i.e.,  $0.09$  arcmin $^{-2}$  mag $^{-1}$  and  $0.11$  arcmin $^{-2}$  mag $^{-1}$ , respectively. Extrapolating the observed counts to beyond the limit where we explicitly reject point-like sources (e.g., 27 mag for CANDELS/DEEP), we estimate a contamination rate of  $\leq 2$ , 5, and  $\leq 2$  sources per field for our  $z \sim 5$ ,  $z \sim 6$ , and  $z \sim 7$  samples from the GN+GS fields,  $<1$  contaminant for our XDF and HUDF09-Ps samples, and  $\sim 1$  contaminant over the BoRG/HIPPIES program. This works out to surface densities of potential stellar contaminants of  $\leq 0.02$ ,  $\sim 0.05$ , and  $\leq 0.02$  arcmin $^{-2}$ , respectively, for our  $z \sim 5$ ,  $z \sim 6$ , and  $z \sim 7$  samples.

Finally, it is also possible that our samples include a small number of contaminant stars even at brighter magnitudes where we exclude pointlike sources or compact sources that significantly prefer a stellar SED. Using simulations similar to those described in Section 4.1 (but for point-like sources with SEDs randomly drawn from the SpeX library), we estimate that our samples would contain at most two such contaminant stars per CANDELS field to  $\sim 27$  mag. Overall, this works out to a contamination rate of  $<1\%$  for our  $z \sim 4$  selections and  $<2\%$  for our  $z \sim 5-8$  samples.

**3.5.2. Transient Sources or Supernovae**

Another potential source of contamination for our high-redshift samples are time-variable events like SNe. Such events could contaminate our samples if observations of sources at bluer and redder wavelengths did not take place over the same time frame and such sources only became bright during observations in the redder bands. Circumstances could then conspire to make such an SN look like a high-redshift star-forming galaxy with a prominent Lyman break, if the SN was sufficiently separated from its host galaxy that it could be identified as a distinct source.

Fortunately, we can easily see from simple arguments that such contaminants will be of negligible importance for our probes. Our explicit exclusion of pointlike sources at bright magnitudes and known SN events (e.g., Rodney et al. 2014) should guarantee that all but the faintest SNe make it in our sample, i.e.,  $\geq 27$  mag (where we no longer exclude point sources). Furthermore, for the CANDELS/WIDE fields where the various epochs of optical and near-IR observations were acquired almost simultaneously (i.e., CANDELS UDS, CANDELS COSMOS, and  $\sim 50\%$  of CANDELS EGS), the

contamination rate will be negligible, as the two epochs are taken within a  $\sim 50$  day timescale, which is short relative to the  $\sim 100$  day decay time for most SN events. Contamination from SNe over the CANDELS/DEEP regions should be similarly low. Owing to the long  $\sim 16$ -month observational baseline, most of the pixels associated with SN brighter than  $\sim 27$  mag would be rejected during the reduction of the WFC3/IR data themselves (or if temporarily brighter than 25 mag identified as an SN by the CANDELS SNe search team; Rodney et al. 2014).

The only scenario where SNe would likely contaminate our selection is if the SNe were likely fading at the time of the initial WFC3/IR observations over the ERS, CANDELS-GN+GS WIDE, or deep-field observations and hence beyond our  $\sim 26.5$  mag limit for rejecting point-like sources over those fields. If we use the approximate SN rate of  $0.03$  SNe arcmin $^{-2}$  derived by Riess et al. (2007) per 40 day period from the GOODS SNe program and use the fact that only  $\sim 40\%$  of SNe would be sufficiently separated from their host galaxy to be identified as an SN (Stroger et al. 2004; Bouwens et al. 2008), we estimate that at most two  $z \sim 7$  galaxies from our program could correspond to SNe. In addition, the lack of any overlap between published SN events (e.g., Rodney et al. 2014) and current  $z \sim 4-10$  catalogs (Section 3.3) provides us with further evidence that the contamination is small.

**3.5.3. Lower-redshift Galaxies**

Are there significant numbers of lower-redshift galaxies in our high-redshift samples? For such galaxies to exist in our samples in large numbers, they would need to have similar colors to  $z \sim 4-10$  galaxies, showing a deep spectral break, blue colors redward of the break, and have relatively small sizes. It is not clear what such objects would be, but low-mass, moderate-age, Balmer break galaxies in the  $z \sim 1-3$  universe are one possibility (e.g., Wilkins et al. 2010), as are intermediate-redshift galaxies with extreme-emission lines (see Section 3.5.4). Dust-reddened intermediate-redshift sources would have far too red colors redward of the break to be included in our high-redshift samples.

Whatever the nature of intermediate-redshift contaminants, they are unlikely to be present in our high-redshift samples, except in very small numbers. Perhaps the most compelling argument for this can be obtained by stacking the flux information in our high-redshift samples. If our samples were significantly contaminated by lower-redshift galaxies, one would expect the stacks of the optical data to show significant detections in the bluest bands. However, deep stacks of our  $z \sim 6$ ,  $z \sim 7$ , and  $z \sim 8$  samples show absolutely no flux in the  $B_{135}$ ,  $B_{135}V_{106}$ , and  $B_{135}V_{106}I_{775}$  bands, respectively, consistent with our high-redshift samples being almost exclusively composed of high-redshift galaxies. In addition, the spectroscopic follow-up done on high-redshift samples reveals very small numbers of lower-redshift contaminants (e.g., Vanzella et al. 2009; Stark et al. 2010).

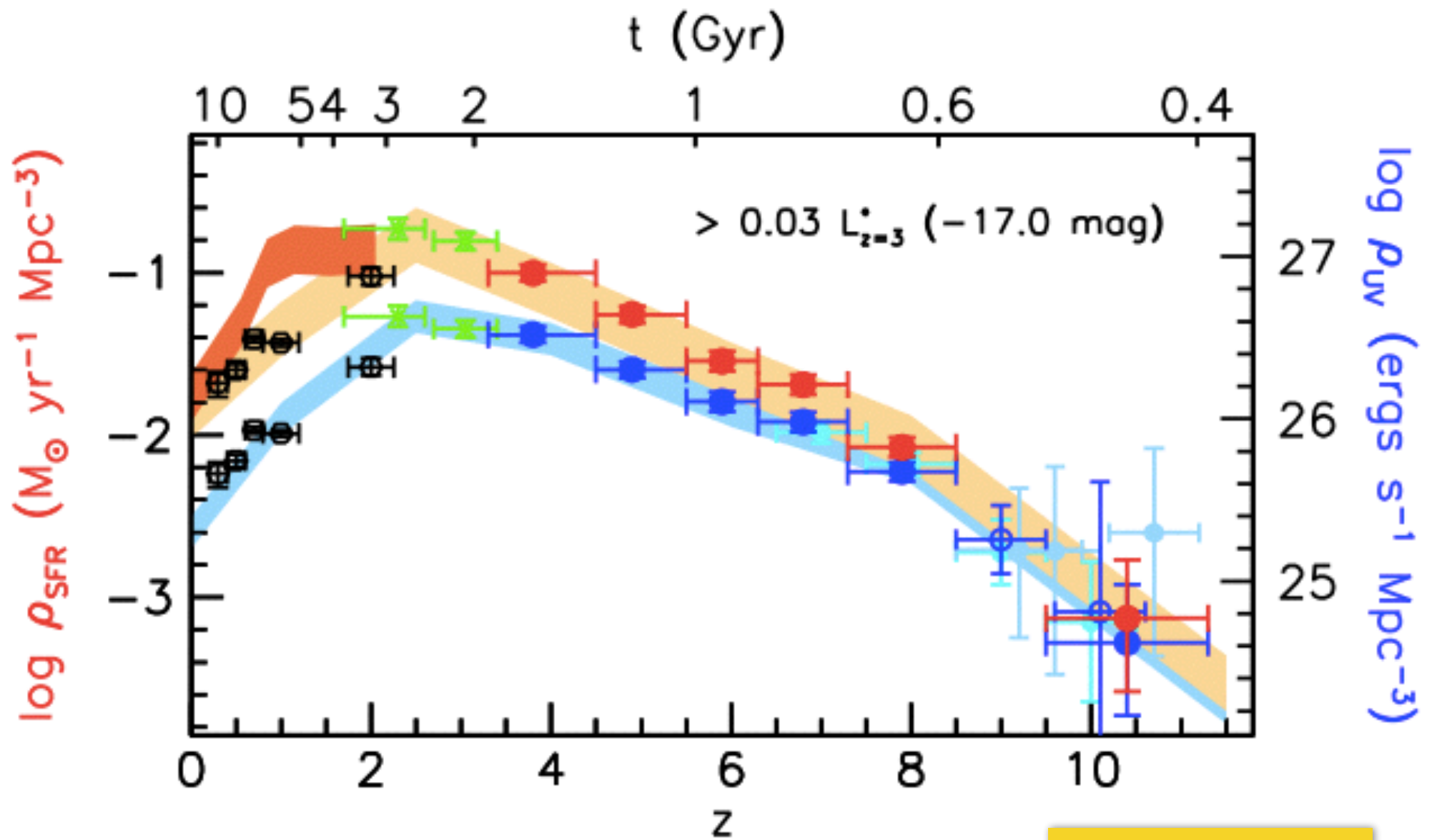
**3.5.4. Extreme Emission Line Galaxies**

Another potential contaminant of our high-redshift samples is so-called extreme emission line galaxies (EELGs), where a significant fraction of the flux from a galaxy is concentrated into a small number of very high equivalent width emission lines (van der Wel et al. 2011; Atek et al. 2011). These

15

# Star-formation density of the Universe

- correct UV luminosity for dust,
- convert into SFR



Bouwens et al. 2015